

1 Exploring Variability in Climate Change projections on the 2 Nemunas River and Curonian Lagoon: coupled SWAT and 3 SHYFEM modeling approach

4 Natalja Čerkasova ^{1,2,*}, Jovita Mėžinė ^{1,*}, Rasa Idzelytė ^{1,*}, Jūratė Lesutienė ¹, Ali Ertürk ^{1,3}, Georg
5 Umgiesser ^{1,4}

6 ¹ Marine Research Institute, Klaipeda University, Klaipeda 92294, Lithuania

7 ² Texas A&M AgriLife Research, Blackland Research and Extension Center, Temple, TX 76502, USA

8 ³ Department of Inland Water Resources and Management, Istanbul University, Istanbul 34134, Turkey

9 ⁴ CNR – National Research Council of Italy, ISMAR – Institute of Marine Sciences, Venice 30122, Italy

10 *Correspondence to:* Jovita Mėžinė, jovita.mezine@ku.lt

11 *Equally contributed: Natalja Čerkasova, Jovita Mėžinė, Rasa Idzelytė

12 **Abstract.** This study advances the understanding of climate projection variabilities in the Nemunas River, Curonian
13 Lagoon, and southeastern Baltic Sea continuum by analyzing the output of a coupled ocean and drainage basin
14 modeling system forced by a subset of climate models. A dataset from a downscaled high-resolution regional
15 atmospheric climate model driven by four different global climate models was bias-corrected and used to set up the
16 hydrological (SWAT) and hydrodynamic (SHYFEM) modeling system. This study investigates the variability and
17 trends in environmental parameters such as water fluxes, timing, nutrient load, water temperature, ice cover, and
18 saltwater intrusions under Representative Concentration Pathway 4.5 and 8.5 scenarios. The analysis highlights the
19 differences among model results underscoring the inherent uncertainties in projecting climatic impacts, hence
20 highlighting the necessity of using multi-model ensembles to improve the accuracy of climate change impact
21 assessments. Modeling results were used to evaluate the possible environmental impact due to climate change through
22 the analysis of the Coldwater fish species reproduction season. We analyze the duration of cold periods (<1.5°C) as a
23 thermal window for burbot (*Lota lota* L.) spawning, calculated assuming different climate forcing scenarios and
24 models. The analysis indicated coherent shrinking of the cold period and presence of the changepoints during historical
25 and different periods in the future, however, not all trends reach statistical significance, and due to high variability
26 within the projections, they are less reliable. This means there is a considerable amount of uncertainty in these
27 projections, highlighting the difficulty in making reliable climate change impact assessments.

28 1 Introduction

29 A river-lagoon-sea continuum is a very complex system that forms a unique and vulnerable environment providing a
30 broad spectrum of the ecosystem services (Kaziukonyte et al., 2021; Inácio et al., 2018) and plays an important
31 socioeconomic role. On the larger scale the climate change impacts are extensively analyzed and already showed that

32 the coastal zone will be impacted by the global warming, sea level rise, by altering of a freshwater runoff, frequency
33 and intensity of coastal storms, precipitation and nutrients patterns (Viitasalo and Bonsdorff, 2022; Lu et al., 2018).
34 Modeling becomes an important tool to project climate change impact with the focus on the intensity and direction of
35 future changes. However, there are a lot of uncertainties regarding the trends and projected impacts due to climate
36 change (IPCC, 2013). The uncertainties and variations of projected future scenarios emerge due to unknowns in global
37 or regional climate models (GCMs, RCMs), proposed scenarios (RCPs), or statistical techniques used for data
38 preparation. Therefore, uncertainty analysis is commonly used to quantify the possible discrepancies between the
39 projections and their impacts on possible future changes. There is a wide variety of studies focused on quantification
40 of climate projection uncertainties around the world, including Lithuania (e.g., Chen et al., 2022; Song et al., 2020;
41 Akstinas et al., 2019). Most of these studies analyze solely hydrological changes due to meteorological input.
42 The uncertainty in climatic studies arises from various factors, as highlighted by Foley (2010). One key factor is the
43 scenario used as the basis for climatic projections. These scenarios range from significantly reduced CO₂ emissions
44 to business-as-usual cases, i.e., continuation of high emissions-based economic growth, leading to vastly different
45 climate trajectories (Latif M., 2011, Taylor et al., 2012). Even if the underlying assumptions are consistent, the climate
46 models used are handling the physics differently leading to different results of the key parameters (Lehner et al., 2020).
47 Apart from the atmospheric models, there is also a variety of ocean models, for example NEMO (Madec et al., 2016),
48 POM (Mellor, 2004), ROMS (Shchepetkin and McWilliams, 2005), MITgcm (Marotzke et al., 1999), SHYFEM
49 (Umgiesser et al. 2004) and others, that have to be considered. All of these models have different discretization,
50 resolution, and representation of the physics modeled. Drainage basin models depend crucially on the changing land
51 use of the basin (Wang et al., 2012, Lin et al., 2015, Waikhom et al., 2023), with subsequent effects on downstream
52 coastal ecosystems.

53 The development of integrated modeling tools is a high-priority task to support the management of the ecosystems at
54 the land-sea interface, prone to both the riverine effects and sea level rise. This study is a continuation of the previously
55 published paper by Idzelytė et al. (2023a) where the framework of coupled hydrological and hydrodynamic models
56 was used to explore the future climate scenarios based on the ensemble mean values for the Nemunas River watershed,
57 Curonian Lagoon, and Baltic Sea continuum. Here, we explore a subset of the possible variation space. We look at
58 different scenarios computed by different climate models, using only one ocean model (Umgiesser et al., 2004) and
59 one drainage basin model (Čerkasova et al., 2018). This allows us to come up with a reasonable estimate of the
60 variability of climate projections and its impact on the hydrology and its application to the ecological evaluation of
61 the studied Nemunas River basin, the Curonian Lagoon, and the southeastern Baltic Sea system as a whole.

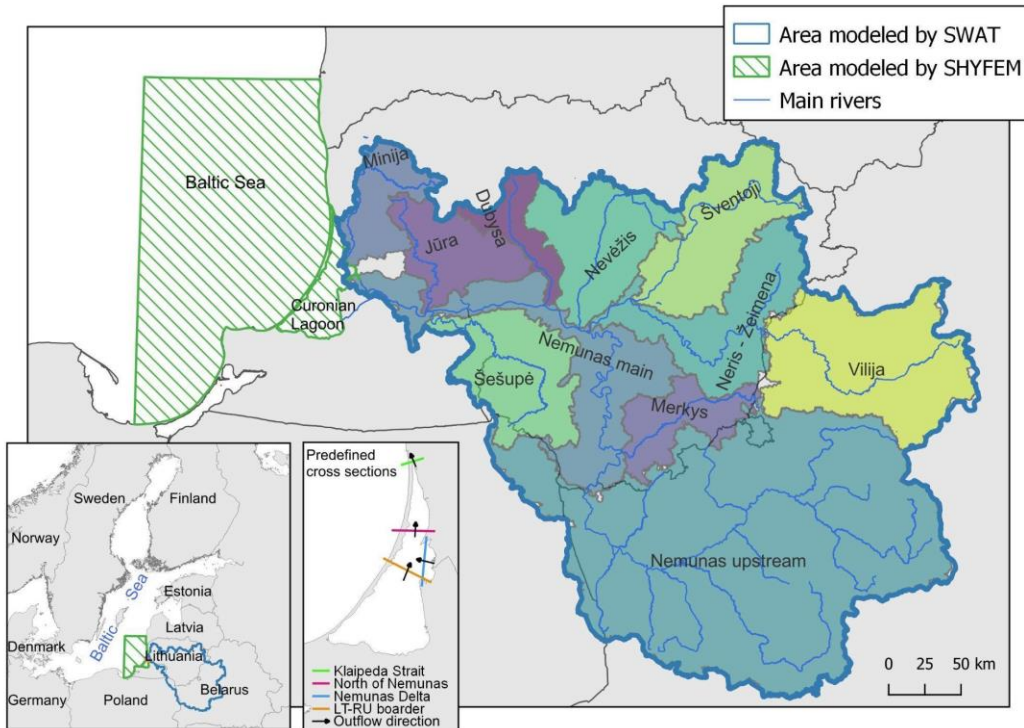
62 It is expected that explicit analysis of the climate scenarios will help decision-makers in the development of climate
63 change adaptation and mitigation strategies as well as adjustment of water quality management, and achievement of
64 regional nutrient policy goals and measures. The level of uncertainty is crucial in the decision-making process,
65 therefore we aim to test model averaging (Idzelytė et al. 2023a) vs. the ensemble method, where we combine the
66 results of several models to form an ensemble projection. The diversity in projections among the ensemble components
67 may reveal the level of variability and aid in combining agriculture nutrient runoff policies with climate mitigation
68 policies that involve integrating strategies to address both issues simultaneously.

69 Climate prediction uncertainty has important implications for the conservation efforts of endangered or vulnerable
70 species, as meteorological-hydrological factors play a primary role in shaping species habitat conditions, life cycle
71 completion, spread, and survival. In addition to the variability in projections for the region, we specifically tackle the
72 question of how much the imposed changes could be reflected in ecosystem function and habitat conditions for the
73 species. As the response of climate forcing is most pronounced in water temperature, we selected the stenotherm
74 species burbot (*Lota lota* L.). As a coldwater fish species, the burbot is particularly sensitive to changes in thermal
75 habitat availability (Harrison et al., 2016) and suffers severe declines throughout its distribution range worldwide
76 (Stapanian et al., 2010). Evaluating the impact of climate change on spawning habitats is essential for projecting the
77 future status of the vulnerable burbot population in the Curonian Lagoon.

78 **2 Materials and methods**

79 **2.1 Study area**

80 Our study site is a large transboundary basin - coastal lagoon - sea system: Nemunas River basin, the Curonian Lagoon,
81 and the southeastern Baltic Sea. The Curonian Lagoon is a shallow estuarine lagoon located in Lithuania and Russian
82 Federation's territory and connected to the south-eastern Baltic Sea through the narrow Klaipėda Strait (Fig. 1). The
83 lagoon covers an area of 1584 km², with its widest section stretching up to 46 km in the southern part. Conversely, in
84 the northernmost part (Klaipėda Strait), it narrows down to approximately 400 m wide. The drainage area of the
85 Curonian Lagoon covers 100 458 km², of which 48% lies in Belarus, 46% in Lithuania, and 6% in the Kaliningrad
86 oblast. Previous hydrodynamic modeling studies revealed that the lagoon consists of two different regions from the
87 water exchange point of view, a transitional region at the northern part of the lagoon and a stagnant southern region
88 which has a considerably higher water residence time. The predominant flow of water is from the south to the north
89 discharging approximately 23 km³ per year into the Baltic Sea.



90
91 **Figure 1. Location of the Curonian Lagoon and Nemunas River Watershed.**

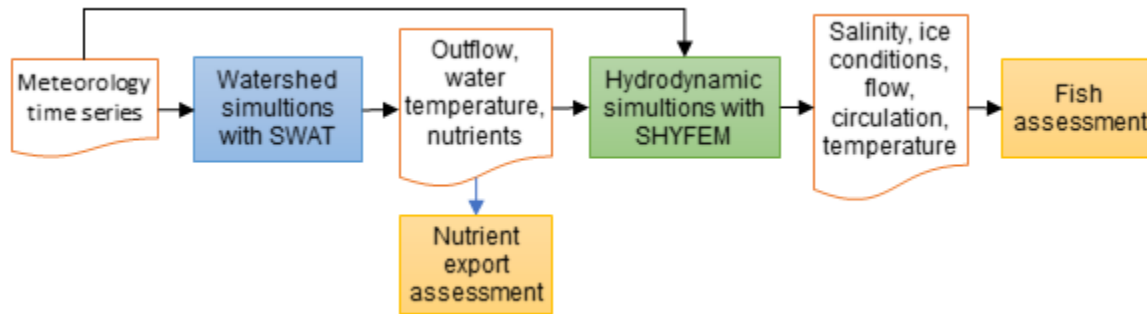
92 The largest river that discharges into the Curonian Lagoon is the Nemunas River, which together with the Minija River
93 brings about 95% of the total riverine input to the lagoon (Zemlys et al., 2013). Both rivers enter the lagoon in the
94 middle of the eastern coast. The average annual discharge of the Nemunas River is 22-24 km³ (Umgiesser et al., 2016)
95 and exhibits a strong fluctuating seasonal pattern, peaking with snowmelt during the flood season in February-April.
96 Due to discharge from the Nemunas River and other smaller rivers, the southern and central portions of the lagoon are
97 considered to be freshwater.

98 The Curonian Lagoon and Nemunas Delta area both include protected territories with various statuses: biosphere
99 polygons, reserves, Natura 2000 (Special Protection Areas (EC Birds Directive), Sites of Community Importance (EC
100 Habitats Directive)) and Ramsar List site (List of Wetlands of International Importance) (Kaziukonyte et al, 2022).
101 The Curonian Lagoon and Nemunas Delta are the most important areas for commercial fishing in Lithuania,
102 contributing about 95-98% of the total inland fishery (Ivanauskas et al, 2022). Bream (*Abramis brama* L.), pikeperch
103 (*Sander lucioperca* L.), and smelt (*Osmerus eperlanus* L.) are the main commercial fish species in the lagoon. In the
104 context of climate change, coldwater species like burbot (*Lota lota* L.) are particularly sensitive. They rely on low
105 water temperatures during winter to initiate the spawning season.

106 2.2 Modeling system

107 Due to limitations in current technology and tools, accurately representing the entire Nemunas River basin, Curonian
108 Lagoon, and southeastern Baltic Sea system at high resolution with a single tool is impossible. As a result, we divided
109 the area and utilized various modeling tools suited for specific purposes, which were coupled together. The modeling

110 system that consists of two main models and numerous utilities mostly developed to transfer the outputs from one
 111 model as inputs to other models are summarized in Fig. 2. The system is characterized by two pivotal models: 1) the
 112 hydrological Soil and Water Assessment Tool (SWAT) model, and 2) the hydrodynamic Shallow water
 113 HYdrodynamic Finite Element Model (SHYFEM). The SWAT and SHYFEM models depict main water flow
 114 dynamics in a Nemunas River watershed-Curonian Lagoon-Baltic Sea continuum.



115
 116 **Figure 2. Hierarchical structure of the modeling system.**

117 The Nemunas River watershed is modeled using the SWAT (Neitsch et al., 2009) which is widely used to simulate
 118 hydrological processes and water quality of watersheds. This model was developed, calibrated, and validated for the
 119 Nemunas River basin in previous studies (Čerkasova et al., 2021, 2019, 2018). The SWAT is a comprehensive tool
 120 that requires numerous model inputs for hydrological parameterization and watershed characterization. The inputs can
 121 differ based on modeling demands and the topographic characteristics of the region. For the Lithuanian part of the
 122 watershed regional high-resolution data (such as the Digital Elevation Model, land use, soil, stream network, reservoir
 123 information) were gathered from the governmental institutions in Lithuania (see Table 1). Where data was not
 124 available, European or global datasets were used, in combination with information found in relevant literature. To
 125 ensure accuracy, we manually digitized the stream network (used as the burn-in layer for watershed delineation and
 126 routing information), reservoir and pond geometry (used to identify the standing waterbody location and for parameter
 127 calculation), and major forest outlines (used to correct the land use layer).

128 Due to the large basin area and heterogeneity in topography and land management in the region, the entire watershed
 129 covering all the Nemunas River Basin was split into separate SWAT sub-models, each representing a sub-watershed
 130 of the main Nemunas River branch. Furthermore, to achieve better parametrisation a separate sub-model represents
 131 the Nemunas and all smaller tributaries situated in the Belarus and Poland territories. The outcome of division into the
 132 sub-models produced the following configuration:

- 133 ● 1 sub-model in the Belarus territory (Neris in Lithuanian, Вілія in Belarus);
- 134 ● 2 transboundary watersheds:
 - 135 ○ Sesupe (Šešupė in Lithuanian, Шешупе in Russian, Szeszupa in Polish);
 - 136 ○ Nemunas upstream (Неман in Russian and Belarus);
- 137 ● 7 sub-models with more than 95% of the territory in the boundary of Lithuania or entirely situated in
 138 Lithuania:

- 139 ○ Minija;
- 140 ○ Merkys;
- 141 ○ Jura (Jūra in Lithuanian);
- 142 ○ Dubysa;
- 143 ○ Sventoji (Šventoji in Lithuanian);
- 144 ○ Nevezis (Nevėžis in Lithuanian);
- 145 ○ Neris- Zeimena (Neris-Žeimena in Lithuanian);
- 146 ● 1 sub-model, - the Nemunas main branch - discharging into the Curonian Lagoon.

147 A total of eleven sub-models were built, subdivided into subbasins (in total 9012), which were further subdivided into
148 Hydrological Response Units (in total 148 212 HRUs), configured, connected, and parametrized. The concept of the
149 eleven SWAT models that are represented as sub-models for the entire study area is given in Figure 1 (denoted as
150 separate colors of the watershed). These models can be used individually or, as in this study, in a framework, where
151 the upstream sub-models provide the input information to the downstream areas. Outputs from the main outlets on the
152 Nemunas and Minija rivers were used as boundary conditions for the hydrodynamic model.

153 Calibration and validation of each sub-model were conducted manually by adjusting parameters linked to specific
154 processes. The multisite calibration process followed an approach typical for hydrological models (Daggupati et al.,
155 2015; Feyereisen et al., 2007). Calibration began with the upstream regions, followed by the downstream areas,
156 focusing on flow, sediment, total nitrogen (TN), and total phosphorus (TP). This methodology was applied both to
157 individual sub-models and the overall modeling framework. Details can be found in Čerkasova et. al (2021).

158 The hydrodynamics of the Curonian Lagoon and the southeastern Baltic Sea were simulated using the open-source
159 shallow water hydrodynamic finite element model SHYFEM, accessible at <https://github.com/SHYFEM-model/> (last
160 accessed on 28 November 2023). The model uses an unstructured grid (finite elements) to discretize the studied basin
161 (Curonian Lagoon and part of the Baltic Sea). The use of finite elements is crucial in order to simulate the narrow
162 connection of the lagoon with the sea (Klaipeda Strait). However, it varies from 250 m close to the Klaipeda Strait to
163 up to 2.5 km in the central part of the lagoon and up to 10 km in the Baltic Proper. The atmospheric forcing has been
164 interpolated directly from the regular grid of the regional climate model data to the finite element nodes by bi-linear
165 interpolation. Lateral boundary conditions have been taken from Copernicus data and interpolated onto the finite
166 element grid (water levels, T, S). The COARE3.0 module is used for bulk formulation. The model solves shallow
167 water equations and, in this study, the 2D version of the model was used. The SHYFEM simulates key physical
168 variables such as circulation, waves, water level, temperature, and salinity fields that are needed to characterize the
169 water matrix. To compute the water fluxes across the sides of the elements, first the conservation of mass in the finite
170 volume around a node that is guaranteed by the continuity equation is used. The fluxes over the lines delimiting the
171 finite volume element per element are made divergence free by subtracting the storage of water inside the node. With
172 these finite volume fluxes the fluxes over the element sides are computed. This tool has been applied to a large number
173 of lagoons around Europe. Details can be found in (Idzelytė et al., 2020, Umgiesser et al., 2016, Zemlys et al., 2013,
174 Umgiesser et al. 2014, and Umgiesser et al. 2004).

175 **2.3 Data**

176 Our modeling system incorporates different input data, varying according to the specific model utilized - either
 177 hydrological or hydrodynamic (as outlined in Table 1). Given that this study follows the research conducted by
 178 Idzelytė et al. (2023a), to delve into the specifics of the input data utilized in our study we refer the reader to their
 179 previously published work.

	Input data type	Source
Hydrological	Digital Elevation Model (DEM)	National Land Service under the Ministry of Agriculture of Republic of Lithuania The Shuttle Radar Topography Mission (SRTM) 1 Arc-Second Global
	Land use and management Data	National Land Service under the Ministry of Agriculture of Republic of Lithuania WaterBase project database Corine landcover 2012 Lithuanian Environmental Protection Agency Eurostat National Statistical Committee of the Republic of Belarus Ministry of natural resources and environmental protection of the Republic of Belarus
	Hydrologic grid	National Land Service under the Ministry of Agriculture The Ministry of Agriculture of the Republic of Lithuania Reports of Belarus government agencies, fishing enthusiasts portals Manual digitization using satellite data
	Soil maps	National Land Service under the Ministry of Agriculture Lithuanian Soil atlas
	Observed discharge and nutrient data	Lithuanian Hydrometeorological Service Lithuanian Environmental Protection Agency
	Crop yield	Lithuanian Statistical Yearbook National Statistical Committee of the Republic of Belarus
	Daily precipitation and air temperature (min/max)	Cordex RCA4 data after bias correction
Hydrodynamic	Water level, temperature, and salinity	RCA4–NEMO model developed by the Rossby Centre and the oceanographic research group at the Swedish Meteorological and Hydrological Institute (SMHI). The bias correction was done by simply adding the difference between the average values of CMEMS and RCA4–NEMO data (Lenderink et al., 2007)
	Bathymetry	The Leibniz Institute for Baltic Sea Research Warnemünde (IOW)
	Ice thickness	ESIM2 model
	Meteorological forcing (wind, pressure, air temperature, solar radiation, cloud cover, precipitation)	Cordex RCA4 data after bias correction
Validation	Precipitation and Air temperature	Lithuanian Hydrometeorological Service (1993-2005), 18 meteorological stations, which are scattered throughout the Republic of Lithuania
	Water level, temperature and salinity	Copernicus Marine Environment Monitoring Service (CMEMS) Baltic Sea Physics Reanalysis product data (1993–2005)

180 **Table 1. Input and validation data types for the hydrological and hydrodynamic modeling system and their respective**
 181 **sources.**

182 Both hydrological and hydrodynamic models were run using the same bias corrected future meteorological forcing
 183 data described in Table 2. Data were obtained from CORDEX (Coordinated Regional Downscaling Experiment)
 184 scenarios for Europe, employing the Rossby Centre high-resolution regional atmospheric climate model (RCA4). This
 185 involved four sets of simulations (downscaling) driven by four global climate models. The datasets are spanning the

186 historical period of 1970–2005 and the projection period of 2006–2100. Projections are based on two Representative
 187 Concentration Pathway (RCP) scenarios, specifically RCP4.5 and RCP8.5 of the Coupled Model Intercomparison
 188 Project Phase 5 (CMIP5). The bias correction was conducted by applying the climate data bias correction tool (Gupta
 189 et al., 2019). The ice thickness data utilized in our study were derived using the ESIM2 model (Tedesco et al., 2009,
 190 Idzelytė and Umgiesser, 2021). This model was run independently as a standalone system, and the resulting output
 191 time series were integrated into our hydrodynamic modeling framework as surface boundary input data. This approach
 192 allowed us to accurately incorporate ice thickness dynamics into our simulations, enhancing the overall reliability of
 193 our model during the ice season. A detailed description of all the data sets used for this study can be found in Idzelytė
 194 et al. (2023a), while the results derived from the modeling system can be found and accessed in the open-access
 195 Zenodo database (<https://doi.org/10.5281/zenodo.7500744>, Idzelytė et al. (2023b)).

Abbreviation	Model	Institution
ICHEC	EC-Earth - A European community Earth System Model	Irish Centre for High-End Computing
IPSL	IPSL-CM5A-LR - Institut Pierre Simon Laplace - Earth System Model for the 5th IPCC report: Low resolution	The Institute Pierre-Simon Laplace
MOHC	HadGEM2-ES - Hadley Global Environment Model 2 - Earth System	Met Office Hadley Centre
MPI	MPI-ESM-LR - Max-Planck-Institute Earth System Mode: Low resolution	Max Planck Institute for Meteorology

196 **Table 2. Meteorological forcing data sources for the hydrological and hydrodynamic modeling system.**

197 2.4 Analysis methods

198 2.4.1 Investigation of hydrological and hydrodynamic model results

199 The analysis was done for the environmental parameters corresponding to our preceding study (Idzelytė et al., 2023a).
 200 These include air temperature, precipitation, Nemunas River discharge, water inflow and outflow from the lagoon at
 201 different locations such as Klaipėda Strait, North of Nemunas, Nemunas Delta, and along the Lithuanian-Russian (LT-
 202 RU) border. In this analysis, we maintained the inflow and outflow categories as in our previous study (Idzelytė et al.,
 203 2023a). We analyzed the data by computing the 10-year moving average using yearly average fluxes, this way ensuring
 204 an accurate representation of water flux dynamics throughout the study period. Water temperature and water level
 205 were evaluated for the Southeast (SE) Baltic Sea and Curonian Lagoon. Saltwater intrusions ($>2 \text{ g kg}^{-1}$) were assessed
 206 in Juodkrantė, approximately 20 km south of Klaipėda Strait. Information on ice cover in the Curonian Lagoon
 207 encompasses the season duration and maximum thickness. Water residence time is analyzed for the northern and
 208 southern parts of the lagoon as well as the total lagoon area.

209 The analysis was done by combining historical (1975-2005) and future scenario projection (2006-2100) periods. That
 210 is, two periods/scenarios were assessed: RCP4.5 and RCP8.5, both ranging from 1975 to 2100. This approach
 211 facilitated a comprehensive assessment of the above-mentioned environmental parameters, enhancing insight into
 212 trends and potential variations over time.

213 In our analysis, we examined the variability of different model runs and the presence of trends and their statistical
214 significance, as indicated by the p -values, across various environmental parameters under different climate models
215 and scenarios. For this, we applied the Mann-Kendall trend analysis (Hussain and Mahmud, 2019). A p -value less
216 than 0.05 was considered statistically significant. The rate of change was quantified using the Theil-Sen estimator
217 (Hussain and Mahmud, 2019). The trend analysis was conducted on model outputs, which were aggregated as yearly
218 means or, in the case of precipitation, as yearly sum.

219 The timing of spring peak flows was estimated by computing a 3-day moving average of the discharge of Nemunas
220 River to the delta region. The day of the maximum value during the typical spring flood window occurrence (from the
221 start of February to the end of April) was noted for each year. The trend was calculated using the same Mann-Kendall
222 trend analysis approach as described above, using the Julian day of peak flow for each year in the simulation period.

223 We analyzed the average annual export of Total Nitrogen (TN) and Total Phosphorus (TP) from the Nemunas River
224 into the Curonian Lagoon. We assessed the trends using the Mann-Kendall test and the 10-year moving averages.
225 These outputs were compared to the Nutrient Ceiling for the Nemunas River requirements outlined in the HELCOM
226 Baltic Sea Action Plan (HELCOM, 2021), which are 29338 t year⁻¹ for TN and 914 t year⁻¹ for TP. We further
227 evaluated the feasibility of meeting these targets under the conditions of different scenarios and climate models.

228 The variability between the models, i.e., uncertainty, was assessed by computing the standard deviation and coefficient
229 of variation using annual values over the entire investigation period (1975-2100). These metrics were based on the
230 yearly average values of modeled parameters (or sum in case of precipitation, ice season duration, and saltwater
231 intrusions) for each of the four simulation results using meteorological forcing data from different climate models.

232 **2.4.2 The possible impact on fish recruitment success**

233 To evaluate the extent and possible impact of climate change on fish recruitment success, the analysis of the burbot
234 spawning period was carried out. Burbot requires very cold temperatures (<2°C) for spawning and egg development
235 (Harrison et al., 2016; Ashton et al., 2019). Within the Curonian Lagoon, it moves to spawning habitats in the Nemunas
236 River delta. Spawning is most intense at the lowest water temperature (close to 0°C) during December-February,
237 usually under ice. The duration of the cold period in the projected time series of temperatures suitable for burbot
238 spawning was calculated by summing days when temperature was below 1.5°C for a given year (days in December
239 were added to the next year). The R package *changept* (Killick and Eckley, 2014, Killick et al., 2022) was used to
240 estimate the number and locations of change points in a time series of cold period duration. The changes in mean and
241 variance at a single point were estimated using the *cpt.meanvar* function, employing the AMOC method. The semi-
242 automatic Pruned Exact Linear Time (PELT) algorithm was employed for the estimation of multiple change point
243 locations, and parameter estimates within segments (time periods). The number of change points was set to five using
244 the parameter Q .

245 **3 Results**

246 **3.1 Ensemble dynamics**

247 **3.1.1 Water flows**

248 There is a noticeable variability among the climate models in terms of the projected mean yearly water fluxes through
249 the predefined lagoon's cross-sections (Fig. 3). Despite this variability, a consistent pattern emerges across all models,
250 with water outflow from the lagoon towards the sea being a prominent feature in every cross-section examined. Each
251 model captures unique hydrodynamic behaviors at different cross-sections of the lagoon. Still, all indicate that the
252 North of Nemunas and Klaipėda Strait cross-sections generally experience higher water fluxes.
253

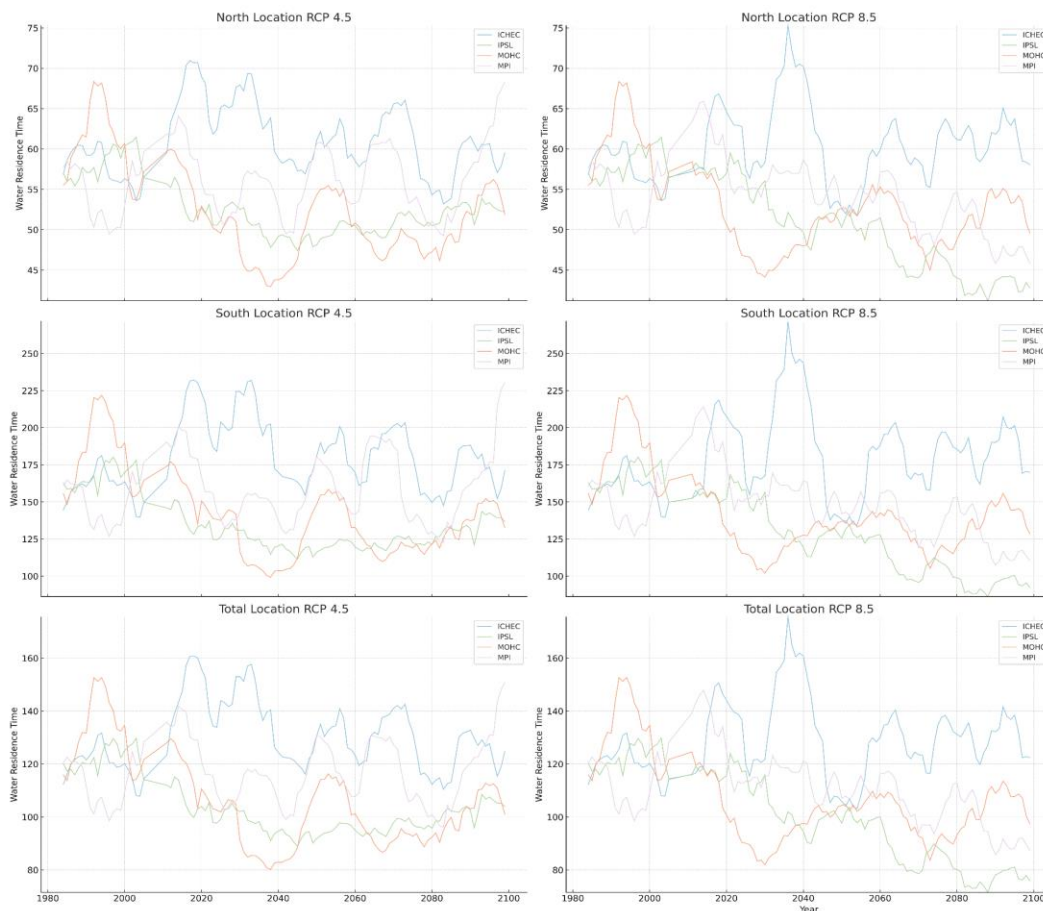


254
255 **Figure 3. 10-year moving average graphs of outflowing (left column) and inflowing (right column) water fluxes (in $m^3 s^{-1}$)**
256 **across four cross-sections within the Curonian Lagoon. Note the adjusted y-axis ranges for fluxes passing through the**
257 **Lithuanian-Russian border.**

258 Across all models, the RCP8.5 scenario consistently results in higher mean outflowing water fluxes compared to
259 RCP4.5, and the MOHC results stand out for consistently projecting the highest mean fluxes in both scenarios,
260 suggesting a more pronounced increase in water movement through the lagoon compared to its counterparts. Both
261 scenarios show a higher outflow to the sea discharge with a possible increase of ~ 300 to $\sim 700 \text{ m}^3 \text{ s}^{-1}$ by the end of
262 the century. These results could lead to the outflow from the lagoon will reach $37.8\text{-}50.4 \text{ km}^3 \text{ year}^{-1}$ which is 24-165
263 % higher compared to historical outflow.

264 Regarding the inflowing water fluxes from the Baltic Sea into the Curonian Lagoon, the IPSL model generally predicts
265 lower fluxes under both scenarios compared to the other models. Inflowing fluxes through the Lithuanian-Russian
266 border show the least variability in predictions across models, especially under the RCP8.5 scenario, indicating a
267 consensus on the water flux through this cross-section.

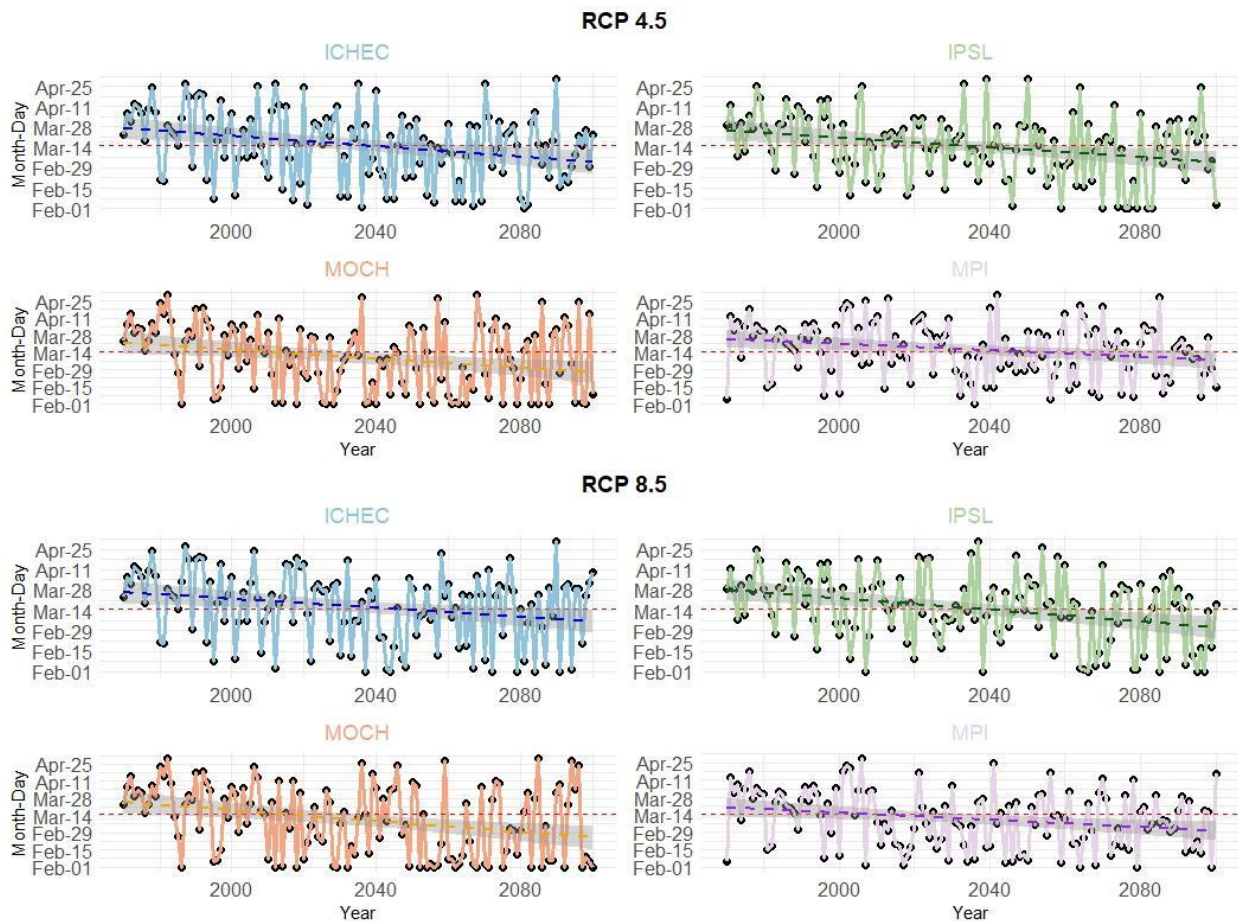
268 Regarding water residence time (Fig. 4 and Appendix A, Fig. A1 and A2), IPSL tends to predict the shortest water
269 residence times, suggesting a model inclination towards faster water turnover in the lagoon. In contrast, ICHEC and
270 MPI, with their higher values, may incorporate factors leading to longer residence times. The shift from RCP4.5 to
271 RCP8.5 and between different analysis areas does not uniformly affect the models.



272
273 **Figure 4. The timing of the annual water residence times (in days) in the North (upper panels), South (middle panels)**
274 **parts of the lagoon and the total lagoon area (lower panels) for both RCPs.**

275 **3.1.2 Timing of peak flows**

276 The high discharge of the Nemunas River and subsequent flooding of the delta region is a nearly annual event which
277 occurs in late winter - spring season and is referred to as “spring flood” in Lithuania. We use the same term in this
278 study and consider the historic period of high river flows to be from 1st of February to 30th of April. The timing of
279 spring floods in the Nemunas River delta was previously reported to shift to earlier days due to climate change
280 (Čerkasova et al., 2021). Further statistical analysis of the projected flows shows that overall there is a statistically
281 significant relationship between the independent variable 'Year' and the Julian day of occurrence of peak flows in the
282 Nemunas River for both RCPs when analyzing the entire period (Fig. 5).

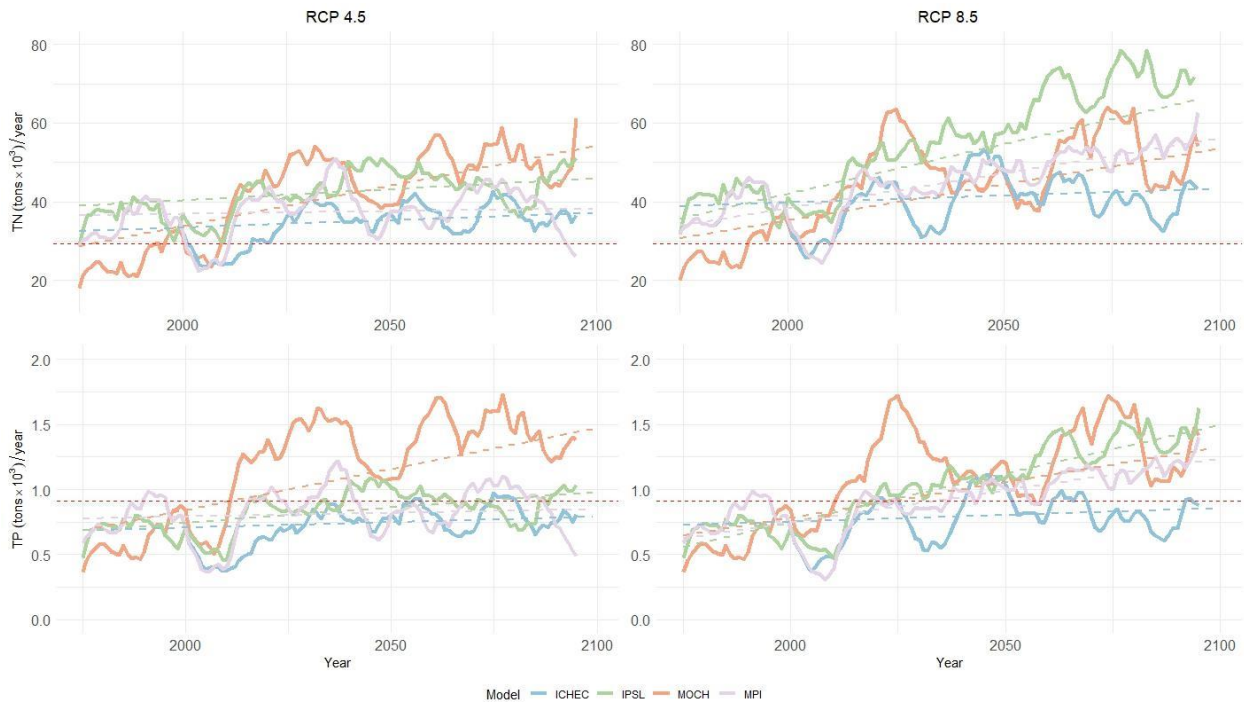


283
284 **Figure 5. The timing of occurrence of the average 3-day maximum flow-rate in the spring (between the 1st of February to**
285 **the 30th of April) of the Nemunas River to the delta region with a trendline for each model. The horizontal red line depicts**
286 **the period's middle date: March 15th.**

287 The graphs show that the projected timing of spring high flows is expected to advance under all climate change
288 scenarios, meaning that the maximum flows are expected to occur earlier in the year. The magnitude of the advance
289 is greater for the higher emissions scenario (RCP8.5). Both IPSL and MOCH project a higher magnitude of change,
290 judging by the steepness of the slope, whereas ICHEC and MPI project a moderate rate of change. This could have
291 several impacts, such as disrupting fish spawning cycles and increasing the risk of flooding.

292 **3.1.3 Nutrient loads**

293 The projections suggest varying levels of variability and trends in the TN and TP loads from the Nemunas River across
294 different RCPs and models (Fig. 6). The RCP8.5 generally projects higher TN and TP loads compared to RCP4.5 for
295 all models. This suggests that more extreme climate change scenarios lead to higher nutrient loads in the study region.



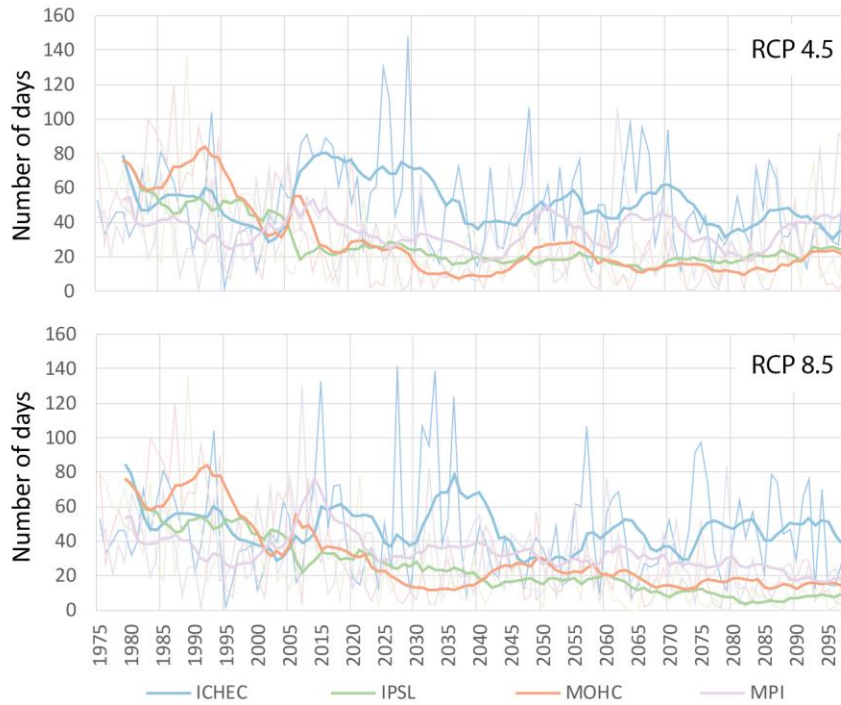
296 **Figure 6. The projected 10-year moving average of the annual mean TN and TP loads from the Nemunas River to the lagoon**
297 **with a trendline for each model. The horizontal red line depicts the Revised Nutrient Input Ceiling for the Nemunas River**
298 **defined by the BSAP update (HELCOM, 2021).**
299

300 The projected TN loads are expected to remain above the Revised Nutrient Input Ceiling under all four climate models
301 and both climate change scenarios (RCP4.5 and RCP8.5) throughout the entire simulation period (shown as a red line
302 in Fig. 6). Overall, the graph suggests that even under the stabilization scenario (RCP4.5), TN loads from the Nemunas
303 River are expected to remain above the BSAP (Baltic Sea Action Plan) targets. Total P loads can fall below the
304 maximum target during several brief periods, but the timing of this will depend on the actual climate scenario that
305 unfolds. There is substantial variability between the models, which indicates a high level of uncertainty in the
306 projections. Notably, under the condition of the MOCH model, the TP projections elevate mid-century and further
307 stabilize at high loads by the end of the modeled period. The IPSL under the RCP8.5 is projecting higher loads,
308 whereas ICHEC and MPI display a moderate increase (Fig. 6). The lowest average annual nutrient load is projected
309 under the ICHEC for both RCPs.

310 **3.1.4 Saltwater intrusions**

311 The data of the number of days of saltwater intrusion events, i.e., when salinity in Juodkrantė exceeds the 2 g kg⁻¹
312 threshold, shows yearly variations across different models (Fig. 7). All models exhibit considerable year-to-year

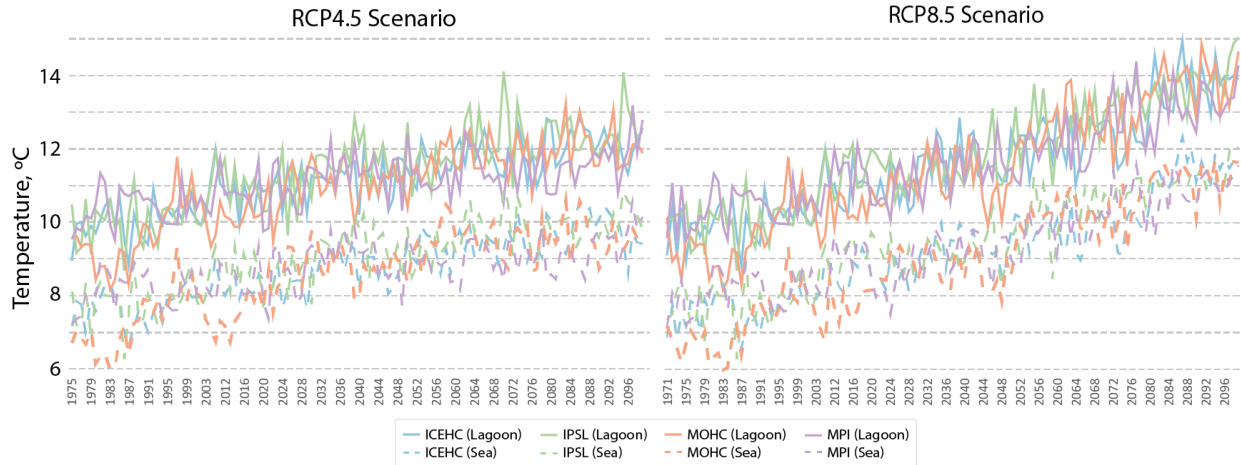
313 variability in the number of saltwater intrusion days, highlighting the complex interplay of climate variability and
314 local hydrological processes affecting the intrusions. Both ICHEC and MPI often show higher numbers of saltwater
315 intrusion days compared to IPSL and MOHC. When comparing the RCP4.5 scenario with RCP8.5, the models yield
316 varying results – ICHEC and IPSL show a slight decrease in intrusion days, MOHC slightly increases, and MPI shows
317 a moderate decrease.
318



319
320 **Figure 7. 10-year moving average of the number of days of saltwater intrusions (salinity exceeding 2 g kg⁻¹ threshold)**
321 **reaching Juodkrantė. Underlying time series denote annual saltwater intrusions.**

322 3.1.5 Water temperature

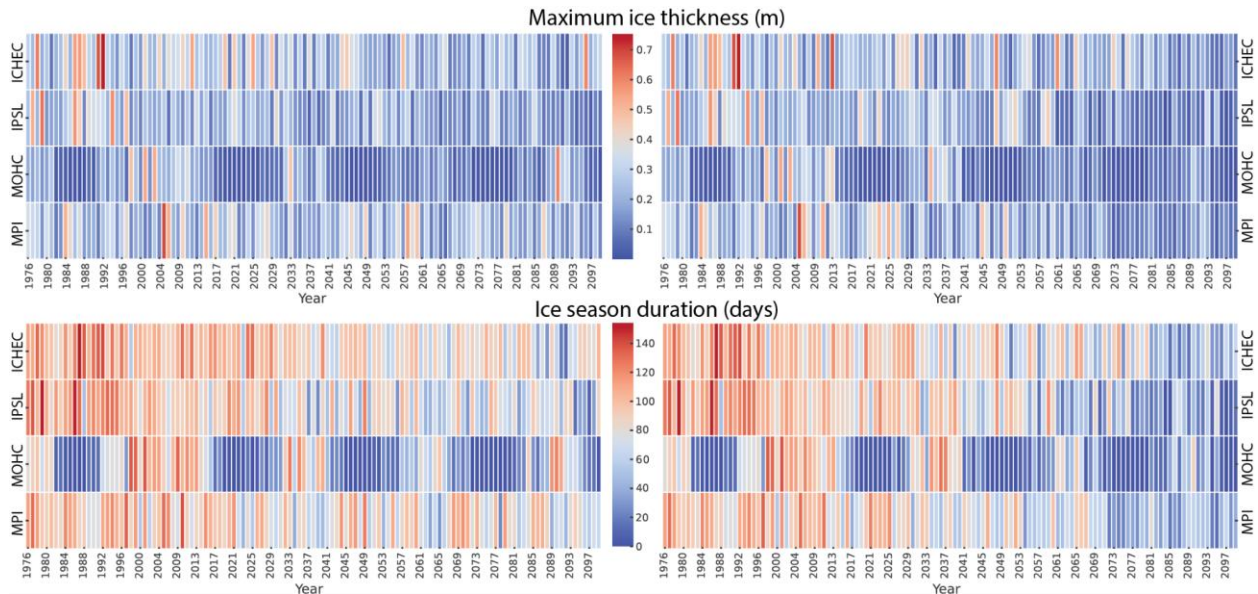
323 The annual mean water temperature within the lagoon and adjacent coastal areas is depicted in Fig. 8. Under the severe
324 RCP8.5 scenario, hydrodynamic model simulations predict a noticeable increase in both mean water temperatures and
325 their variability compared to the RCP4.5 scenario, indicating higher temperatures with greater uncertainty ahead. The
326 IPSL model consistently projects slightly warmer temperatures across scenarios, while the MOHC model shows the
327 largest jump in variability, suggesting that it predicts greater uncertainty under RCP8.5. Despite model variations, the
328 trend towards warmer and more uncertain climate conditions is universally acknowledged.



329
 330 **Figure 8. 10-year moving average of annual mean water temperature in the Curonian Lagoon and southeastern coastal**
 331 **area of the Baltic Sea.**

332 **3.1.6 Ice thickness**

333 The comparative analysis of climate model projections for maximum ice thickness and ice season duration (Fig. 9)
 334 highlights the diverse outcomes projected by different model simulations over time and through various scenarios. All
 335 models indicate a shortening of the ice season and thinning of the ice. Notably, the MOHC model often showed lower
 336 thicknesses and shorter ice season duration compared to other models with a distinctive sinusoidal pattern. In contrast,
 337 ICHEC indicates a more gradual decline in ice season duration, whereas IPSL and MPI exhibit a greater variability
 338 over the years. Regarding maximum ice thickness, ICHEC and MPI show higher year-to-year variability.




339
 340 **Figure 9. Heatmaps of maximum ice thickness and ice season duration in the Curonian Lagoon. RCP4.5 (left) and RCP8.5**
 341 **(right).**

342 **3.2 Trend analysis**

343 Figure 10 provides a comprehensive overview of trends, accompanied by their statistical significance (*p*-values), and
 344 the rate of change (Theil-Sen estimator) for various environmental parameters under different climate scenarios. The
 345 results revealed that numerous parameters exhibited significant trends over time. Notably, air temperature and
 346 precipitation consistently show significant increasing trends in all scenarios. Although the rate of change varies among
 347 the climate models, precipitation exhibits a more pronounced increase compared to air temperature. Water temperature
 348 and water level also consistently exhibit increasing trends in all scenarios.
 349

Parameter	Presence of trend and its significance (p-value)										The rate of change (Theil-Sen estimator)									
	Historical + RCP 4.5					Historical + RCP 8.5					Historical + RCP 4.5					Historical + RCP 8.5				
	Model					Model					Model					Model				
	ICHEC	IPSL	MOHC	MPI	Mean	ICHEC	IPSL	MOHC	MPI	Mean	ICHEC	IPSL	MOHC	MPI	Mean	ICHEC	IPSL	MOHC	MPI	Mean
Air temperature (°C)	<0.01	<0.01	<0.01	<0.01	<0.01	<0.01	<0.01	<0.01	<0.01	0.02	0.03	0.03	0.03	0.02	0.03	0.04	0.05	0.05	0.03	0.04
Precipitation (mm year ⁻¹)	<0.01	<0.01	<0.01	0.02	<0.01	<0.01	<0.01	<0.01	<0.01	<0.01	1.00	1.64	1.48	0.68	1.21	0.90	3.21	2.14	2.07	2.08
Water outflow from the lagoon (m ³ s ⁻¹)	0.04	<0.01	<0.01	0.35	<0.01	0.01	<0.01	<0.01	<0.01	<0.01	1.19	2.34	6.41	0.59	2.72	1.57	6.68	6.08	4.32	4.79
	0.02	<0.01	<0.01	0.37	<0.01	0.01	<0.01	<0.01	<0.01	<0.01	1.20	2.31	6.21	0.57	2.67	1.56	6.50	5.91	4.20	4.68
Nemunas Delta	0.03	<0.01	<0.01	0.46	<0.01	0.01	<0.01	<0.01	<0.01	<0.01	0.85	2.13	4.83	0.41	2.11	1.26	5.58	4.60	3.44	3.79
	<0.01	<0.01	<0.01	<0.01	<0.01	<0.01	<0.01	<0.01	<0.01	<0.01	0.56	0.62	2.82	0.46	1.13	0.69	1.73	2.93	1.34	1.67
LT-RU border	0.47	<0.01	0.02	0.19	0.01	0.57	<0.01	0.32	<0.01	<0.01	-0.16	-0.75	-0.41	0.22	-0.25	-0.11	-1.39	-0.27	-0.46	-0.54
	0.50	<0.01	0.01	0.25	0.01	0.66	<0.01	0.01	<0.01	<0.01	-0.16	-0.77	-0.57	0.21	-0.28	-0.09	-1.52	-0.42	-0.57	-0.64
Water inflow from the sea (m ³ s ⁻¹)	0.38	0.20	0.74	0.02	0.98	0.97	0.07	0.83	0.33	0.70	-0.10	-0.15	-0.05	0.21	0.00	0.00	-0.21	-0.04	0.11	-0.03
	0.38	<0.01	<0.01	0.03	<0.01	0.37	<0.01	<0.01	1.00	<0.05	0.11	-0.25	0.88	0.35	0.28	0.13	-0.57	1.11	0.00	0.05
Max spring flow (Julian day)	<0.01	<0.01	<0.01	<0.01	<0.01	<0.01	<0.01	<0.01	<0.01	<0.01	-0.18	-0.17	-0.20	-0.15	-0.28	-0.14	-0.19	-0.23	-0.15	-0.28
Nutrients (T year ⁻¹)	0.01	<0.01	<0.01	0.09	<0.01	0.04	<0.01	<0.01	<0.01	<0.01	65.16	121.62	287.07	49.20	57.11	65.94	388.51	251.99	217.60	88.94
	0.03	<0.01	<0.01	0.14	<0.01	0.07	<0.01	<0.01	<0.01	<0.01	1.69	3.23	9.41	1.28	3.68	1.66	9.04	7.48	5.72	6.23
Total Phosphorus	0.01	<0.01	<0.01	0.47	<0.01	0.01	<0.01	<0.01	<0.01	<0.01	1.09	2.30	4.80	0.51	2.11	1.37	5.71	4.39	3.59	3.73
Nemunas River discharge (m ³ s ⁻¹)	<0.01	<0.01	<0.01	<0.01	<0.01	<0.01	<0.01	<0.01	<0.01	0.01	0.02	0.02	0.03	0.01	0.02	0.03	0.03	0.04	0.03	0.03
Water temperature (°C)	<0.01	<0.01	<0.01	<0.01	<0.01	<0.01	<0.01	<0.01	<0.01	<0.01	0.02	0.02	0.03	0.01	0.02	0.03	0.04	0.04	0.03	0.04
	<0.01	<0.01	<0.01	<0.01	<0.01	<0.01	<0.01	<0.01	<0.01	<0.01	-0.51	-0.49	-0.27	-0.23	-0.40	-0.60	-0.56	-0.32	-0.41	-0.53
Burbot spawning period (days, t<1.5°C)	<0.01	<0.01	<0.01	<0.01	<0.01	<0.01	<0.01	<0.01	<0.01	<0.01	0.20	0.09	0.98	0.16	0.36	0.27	0.15	1.07	0.21	0.42
	<0.01	<0.01	<0.01	<0.01	<0.01	<0.01	<0.01	<0.01	<0.01	0.03	0.21	0.12	1.00	0.16	0.37	0.28	0.24	1.07	0.25	0.46
Water level (cm)	<0.01	<0.01	0.02	<0.01	<0.01	<0.01	<0.01	<0.01	<0.01	<0.01	-0.35	-0.53	-0.17	-0.25	-0.29	-0.59	-0.87	-0.28	-0.60	-0.64
	<0.01	<0.01	0.17	0.09	<0.01	<0.01	<0.01	<0.01	<0.01	<0.01	-0.11	-0.13	-0.03	-0.04	-0.09	-0.12	-0.17	-0.06	-0.14	-0.14
Ice	0.07	<0.01	<0.01	0.95	<0.01	0.18	<0.01	<0.01	<0.01	<0.01	-0.16	-0.29	-0.39	0.00	-0.38	-0.11	-0.43	-0.40	-0.19	-0.45
Salinity in Juodkrantė >2 g kg ⁻¹ (days)	0.87	0.03	<0.05	0.40	0.18	0.64	<0.01	0.01	<0.01	<0.01	0.01	-0.06	-0.08	0.03	-0.02	0.02	-0.16	-0.06	-0.09	-0.08
	0.55	<0.01	0.03	0.64	0.08	0.33	<0.01	0.01	<0.01	<0.01	0.09	-0.29	-0.36	0.07	-0.12	0.15	-0.72	-0.27	-0.38	-0.36
Water residence time (days)	0.68	0.01	0.02	0.56	<0.05	0.47	<0.01	0.03	<0.01	<0.01	0.04	-0.18	-0.24	0.06	-0.08	0.07	-0.47	-0.19	-0.25	-0.24

350 

351 **Figure 10. Mann-Kendall trend analysis results. Trends and their significance (p-values assessed at a 0.05 confidence level)**
 352 **with their rate of change (Theil-Sen estimator) of key environmental parameters throughout historical and RCP4.5 and 8.5**
 353 **scenarios in different geographical locations within the Curonian Lagoon and southeastern (SE) Baltic Sea. Cells are**
 354 **colored based on the direction of the trend.**

355 The MPI model exhibited the most frequent instances of statistically insignificant trends across the projected
 356 parameters. Notably, water inflow/outflow, nutrient discharge, riverine discharge, ice thickness, salinity, and water
 357 residence times all failed to meet the *p* < 0.05 significance threshold. Interestingly, the MPI model produced the
 358 highest *p*-value (0.02) for precipitation, which is the primary driver of other hydrological and hydrodynamic conditions
 359 in the model. It is worth noting that if the threshold for statistical significance were further reduced (e.g., *p* < 0.01),
 360 the results for the MPI model could be entirely dismissed. This highlights the importance of carefully considering the
 361 chosen significance level when interpreting model outputs.

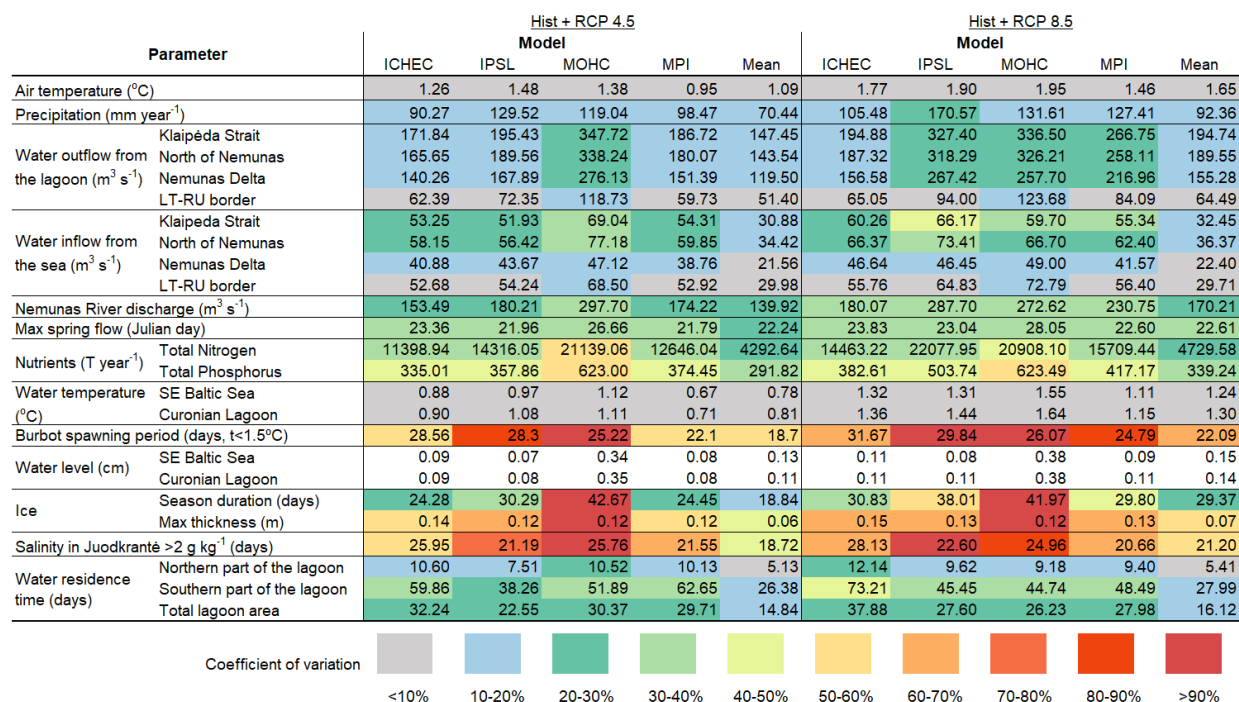
362 Theil-Sen slope estimates reveal a consistent pattern of increasing river discharge, nutrient loads, and water outflow
 363 across all projections. Conversely, consistent with these rising outflows, negative slopes were observed for inflows

364 from the sea and salinity. These findings collectively suggest a projected increase in freshwater input to the Curonian
 365 Lagoon, potentially impacting its biological communities.

366 Figure 10 highlights a critical limitation of analyzing ensemble means alone: it can obscure the heterogeneity present
 367 within individual model projections. This is evident in the water inflow at the LT-RU border, where two models show
 368 statistically insignificant trends, yet the ensemble mean indicates a significant trend. Similarly, the individual model
 369 slopes for IPSL (-0.25) and ICHEC (0.88) portray contrasting projections (decrease vs. increase) compared to the
 370 ensemble mean (0.28) which leans towards an increase. These observations emphasize the importance of considering
 371 the spread of individual model projections and their uncertainties, rather than solely relying on the ensemble mean.

372 3.3 Variability in the projections

373 Analysis of standard deviations (SD) offers a comprehensive insight into the variations across simulation results using
 374 forcing from different climate models, while coefficients of variation (CV) provide a standardized measure of relative
 375 variability across the assessed environmental parameters (Fig. 11). Air and water temperatures have relatively low SD
 376 values. However, the deviation is more pronounced under the RCP8.5 scenario. Additionally, the SD is higher for air
 377 temperature compared to water temperature. In the case of precipitation, the SD presents more diverse results between
 378 the models, adding to the uncertainty of the modeling results.



379
 380 **Figure 11. Standard deviations of key environmental parameters throughout historical and RCP4.5 and 8.5 scenarios in**
 381 **different geographical locations within the Curonian Lagoon and southeastern (SE) Baltic Sea. Cells are colored based on**
 382 **the coefficient of variation.**

383 The low p -values (Fig. 10) indicate that the trends in earlier maximum spring flows are statistically significant.
384 Variability in the SD values across models and RCPs (Fig. 11) suggests that there is uncertainty associated with these
385 projections. The range of Theil-Sen slopes also indicates variability in the rate of decline in the timing of maximum
386 spring flows across different scenarios. Therefore, while the trends are significant, the variability in the projections
387 should be considered when interpreting and using these results for decision-making. The SD values for the occurrence
388 of maximum spring flows range from 21.79 (in the MPI 4.5 scenario) to 28.05 days (in the MOHC 8.5 scenario),
389 where higher SD values indicate greater variability in the predicted time series data. Both IPSL and MPI models have
390 lower prediction variability, whereas MOHC and ICHEC display larger variability. The RCP8.5 scenario indicates a
391 greater degree of change, consistent with previous studies (Idzelytė et al., 2023a, Čerkasova et. al., 2021). For both
392 RCP4.5 and RCP8.5, the MPI model has the lowest CV (29% and 32%), while the MOHC model has the highest CV
393 (38% and 40%). Based on these results it can be concluded that the MPI model appears to be less variable compared
394 to the other models for both RCP4.5 and RCP8.5 scenarios. Conversely, the MOHC model appears to be more variable
395 compared to the other models for both scenarios.

396 Analysis of potential future TN and TP loads in the Nemunas River reveals a broad spectrum of possibilities. The
397 variation is linked to the specific climate model and RCP scenario chosen. However, a consistent trend emerges across
398 all models and RCPs – an upward trajectory for nutrient loads. Anthropogenic activities are the primary driver of
399 nutrient loading from land sources. While climate factors, such as increased precipitation and subsequent nutrient
400 wash-off, might exert a net negative impact on loads, a comprehensive future outlook requires incorporating
401 anticipated changes in nutrient management practices and land use. This study acknowledges the omission of these
402 factors, highlighting the need for further analysis to identify the most probable scenario and develop potential
403 mitigation strategies for nutrient pollution in the Nemunas River.

404 When examining water dynamics within the lagoon, areas with greater fluctuations in SD are notably found in regions
405 where water flow is more intense. This pattern is particularly distinguished from the Nemunas Delta going northward
406 to the Klaipėda Strait. Variability is much higher for water outflow than inflow. The most significant variation between
407 the models is evident under the RCP4.5 scenario, where simulation results derived using MOHC datasets produce
408 much higher SD than other models. A similar pattern is also evident for the ice season duration, while SD for saltwater
409 intrusions in the lagoon is relatively similar between the different models. Water residence time exhibits the same
410 variability between the models in all analysis sections. Notably, the IPSL model demonstrates a lower SD under the
411 RCP4.5 scenario, while the ICHEC model exhibits a higher SD under the RCP8.5 scenario.

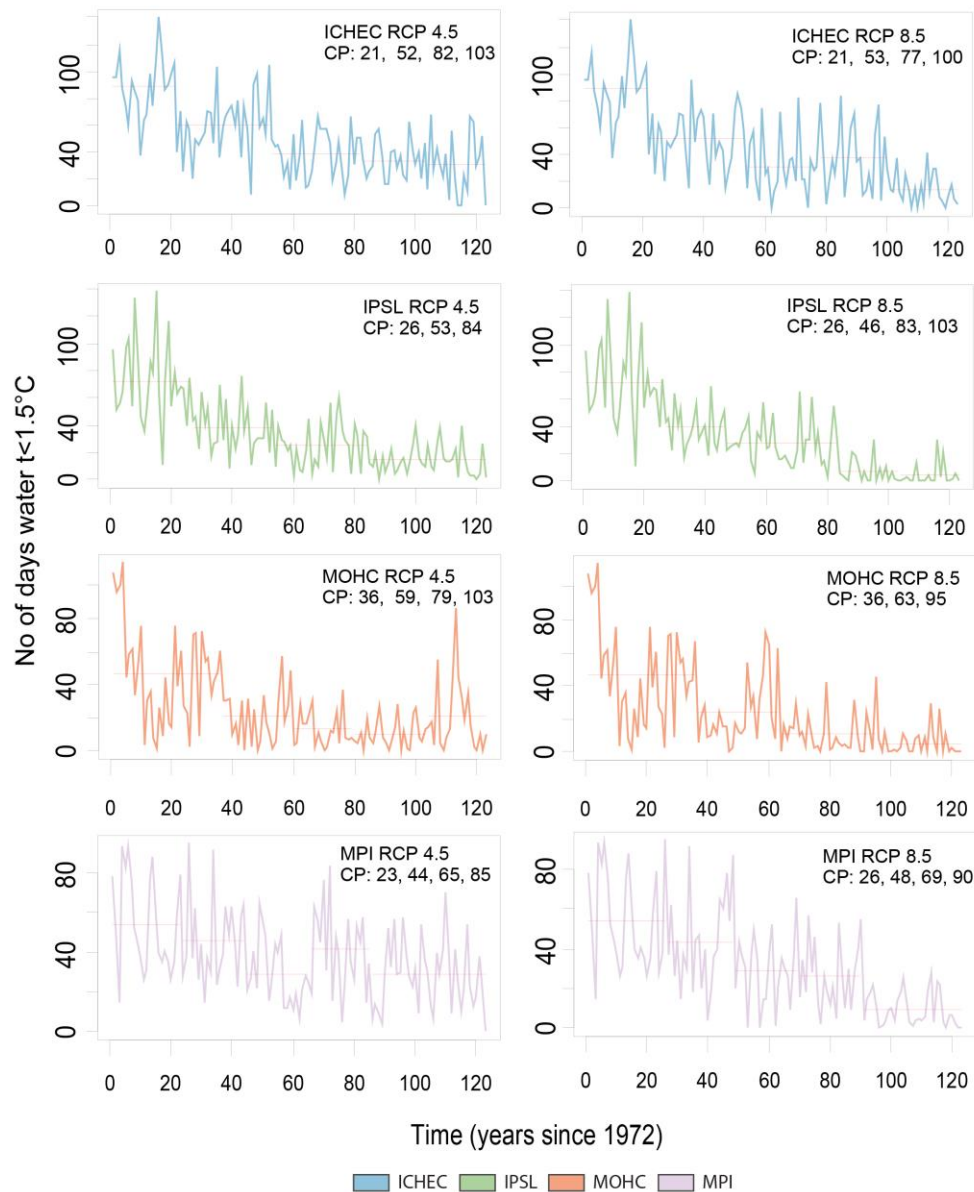
412 In almost all instances, except for water level, the SD statistics derived from the model-averaged datasets exhibit lower
413 values. This suggests a reduction in variability compared to individual models, emphasizing the smoothing effect
414 achieved through model averaging. The most pronounced disparity in SD among the models is observed in the case
415 of MOHC, particularly regarding the RCP4.5 scenario.

416 The differences between climate models become more apparent when considering coefficients of variation. While air
417 and water temperatures show relatively consistent results with low CV values, parameters like salinity and ice-related
418 variables display higher CV values, highlighting greater variability and uncertainty among the climate models. Among
419 the parameters indicating water flow dynamics in different areas of the Curonian Lagoon, again a clear disparity of

420 the MOHC model can be seen. This indicates the model's distinct response and emphasizes the need for careful
421 consideration when employing the data of this climate model in hydrodynamic and hydrological simulations.

422 **3.4 Changepoint analysis of burbot spawning period time series**

423 The single changepoint analyses of major shifts in mean and variance in time series of the duration of the cold season
424 suitable for burbot spawning occur from 2013 to 2029 according to modeling results of RCP4.5 (Appendix B Fig.
425 B1). The mean value of the time segment involving historical and recent past varies from 47 (MOHC RCP4.5) to 72
426 days (ICHEC RCP4.5). In the next period, it becomes shorter by 66% according to MOHC and IPSL models and by
427 36 and 51% according to MPI and ICHEC models, respectively, taking no longer than one month. In three of the four
428 RCP8.5 scenario models the single changepoint could only be detected at the end of the time series, after 2040-2060
429 when the cold period duration is reduced to 6 to 9 days. An exception was generated by ICHEC RCP8.5 model results,
430 indicating a changepoint in the historical past, showing that the duration of the cold period already decreased by 60%
431 in 1992 (Appendix B Fig. B1). Somewhat surprisingly, no changepoints in terms of variance are detected in the IPSL
432 and ICHEC time series. Change in variance was detected in the IPSL time series in 1995 and in the MOHC time series
433 in 2003 and 2013 (Appendix B Fig. B2), so both occurred within the historical period. Both model results indicate a
434 2 to 3 times higher variance of the cold period duration in the historical period than post changepoint period (Appendix
435 B Fig. B2).



436
 437 **Figure 12. Changepoint (CP) detection in the modeled time series of burbot spawning period $t < 1.5^{\circ}\text{C}$ duration (Vente area).**
 438 **CP refers to changepoints indicated in a number of years since 1972.**

439 Multiple changepoint detection analyses indicated three to four changepoints in the modeled time series of cold period
 440 duration (Fig. 12). The significant decrease in a mean number of $< 1.5^{\circ}\text{C}$ days occurred in the 1990s according to MPI,
 441 IPSL, and ICHEC models, and the change was particularly obvious in the results of IPSL and ICHEC models 46-47%
 442 and 33-42% reduction, respectively (Table 3). The cold period duration decreased from three to two months according
 443 to the ICHEC RCP4.5 model and even to less than 2 months in ICHEC RCP8.5 in 1992. The next time segment where
 444 all modeled time series had a changepoint is close to the present time and near future (Table 3). After this changepoint
 445 the cold period is further shrinking. If in the 1990s the MPI model showed only a slight decrease in the number of
 446 cold days (15%), after 2021 (MPI RCP4.5) and 2025 (MPI RCP8.5) the reduction is more severe (46%). After the

447 second changepoint, 46 to 72% of the initial cold period duration is lost according to all model results. According to
 448 three out of four model results, the cold period duration is less than one month after the 2030s.

	Change points & Means of periods								
	Mean I	Historic CP	Mean II	Present & Near future 2020-2040 CP	Mean III	Long- term 2040- 2060 CP	Mean IV	Long- term >2060 CP	Mean V
MOHC 4.5	47	2013	20	2036	13	2056	10	2080	21
MPI 4.5	54	1994	46	2021	29	2042	42	2062	29
IPSL 4.5	72	1997	38	2030	25	-	25	2061	14
ICHEC 4.5	89	1992	60	2029	38	2059	34	2080	30
MOHC 8.5	46	2013	24	2040	11	-	11	2072	5
MPI 8.5	54	1997	43	2025	29	2046	26	2067	9
IPSL 8.5	72	1997	39	2023	28	2060	7	2080	5
ICHEC 8.5	89	1992	52	2030	31	2054	37	2077	14

449 **Table 3. Multiple changepoints (CP, years) in modeled time series and mean values of burbot spawning period duration**
 450 **(number of days when the temperature was <1.5 °C) in subsequent periods (I-V) at the Vente area.**

451 **4 Discussion**

452 Variability and uncertainty are not a flaw but a representative aspect of predicting complex systems. Multi-model
 453 ensembles (MMEs) are a vital tool in managing this uncertainty, providing a more robust and reliable basis for
 454 understanding future climate conditions and informing global efforts to mitigate and adapt to climate change. One
 455 common method to analyze MMEs for climate change impact assessment is ensemble averaging, which is often
 456 considered more accurate than any individual model's prediction, smoothing out model-specific biases. We performed
 457 this type of research in our previous study (Idzelytė et al., 2023a), however, investigating the dynamics of each model
 458 separately is important for evaluating the overall variability in impact predictions since relying only on multi-model
 459 averaging can obscure the detailed representation of extreme values and the variability of the parameters under study,
 460 potentially affecting the accuracy of projections (Tegegne et al., 2020).

461 In our study, 2 RCPs model scenarios of one RCM driven by 4 GCM were analyzed and each model showed
 462 independent variability of the parameters and its trends. In general, the trends are aligned in the same trajectory but
 463 the slope differs: sharper decreases or increases occur in data series based on RCP8.5 forcing. Our study also indicates
 464 that even under climate mitigation scenario RCP4.5 the changes in hydrological processes and temperature regimes
 465 are significant. The combined analysis of standard deviations and coefficients of variation provides valuable insights
 466 into the divergences between climate models in simulating hydrodynamic and hydrological processes.

467 **4.1 Riverine inputs and water flows**

468 The discharge of the Nemunas River exhibits a pronounced and statistically significant increasing trend, accompanied
469 by escalating rates of change. The overall water outflow from the lagoon also reveals increasing trends suggesting
470 changes in hydrological patterns, while water inflow varies in significance across scenarios and locations. The
471 significance of the latter is inconsistent and varies between different climate models, with some of them (depending
472 on the cross-sections) displaying no significant trends, and others indicating a decrease in water inflow.

473 Results from the 10-year moving average imply much higher variability between the models in the long-term period,
474 which reveals the cumulative effect of the uncertainties and complexity of the system. Our study results differ greatly
475 compared to Jakimavičius et al. (2018) study based on the IPCC (2013) climate models without downscaling (GFDL-
476 CM3, HadGEM2-ES, NorESM1-M). Jakimavičius et al. (2018) study applied the HBV hydrological model and used
477 statistical methods to calculate the Baltic Sea parameters. With these techniques the main following projected outputs
478 were generated: 1) the Nemunas outflow decrease from 22.1 to 15.9 km³ with RCP8.5 scenario; 2) decreasing trend
479 of the outflow to the sea will induce only 0.7% from the reference value; 3) and significant inflow increase to the
480 lagoon due to sea level rise was calculated up to 61.3% higher compared to the reference period (Jakimavičius et al.,
481 2018).

482 Our study results are in line with Plunge et al. (2022) where the SWAT model with 7 regional climate models was
483 applied to test RCP4.5 and RCP8.5 scenarios. Plunge et al. (2022) study projected the increase of the Nemunas River
484 discharge by 9.7% for RCP4.5 and by 35.4% for the RCP8.5 scenario by the end of the century. The divergent results
485 from various studies show the necessity to evaluate climate change scenarios with care. The use of the regional-bias
486 corrected data has a minor variation in the near future; however, the long-term projections are still uncertain. The trend
487 analysis showed that the MOHC model projected the highest riverine input, as a result, most of the other parameters
488 had more distinguished results compared to other models.

489 The associated trends in water residence time (WRT) in different parts of the lagoon are diverse, having varying levels
490 of significance and rates of changes. However, most of the RCP4.5 models did not show significant trends except the
491 mean trend for this scenario, while with RCP8.5 models prevailing trends of decreasing water residence time can be
492 observed. The decreasing trends can be explained by the higher Nemunas discharges and the increased outflow from
493 the lagoon to the sea. Moreover, the timing of the maximum spring flood shifting to earlier days in the year could have
494 important implications for the lagoon flushing rate in spring, e.g., the absence of ice jam could profoundly reduce the
495 likelihood of the sudden water level rise and extreme flood event risk. Earlier spring floods and the tendency of shorter
496 WRT in the lagoon could have important implications for biogeochemical cycles, nutrient regimes, and associated
497 phytoplankton primary production peaks and overall nutrient retention capacity. The projections show that the timing
498 of spring high flows are moved to the boundary of the analyzed period (February 1st), which indicates that the peak
499 flow rate might occur even earlier in the year. Although not analyzed in this paper, a follow-up study will explore
500 these projections using more appropriate methods for detecting trends in flood timing, i.e. using the circular statistics
501 approaches (Blöschl et al., 2017).

502 **4.2 Saltwater intrusion into the freshwater system**

503 The variability of water inflow from the Baltic Sea into the lagoon impacts saltwater intrusions in the northern part of
504 the lagoon and has significant effects in the area, extending to around Juodkrantė, which is situated approximately 20
505 kilometers southward of the Klaipėda Strait (sea inlet). The duration of saltwater intrusions in this specific area
506 exhibits varying trends and rates of change, with certain scenarios displaying significant decreases in the number of
507 days per year when salinity exceeds 2 g kg^{-1} , while others – no significant changes. Analysis of single-model saltwater
508 intrusions showed huge variability between the years, particularly it can be visible in ICHEC and MPI model
509 projections. The large variabilities of the projected future salinity were discussed in other studies as well (Meier et al.,
510 2022a, 2022b), claiming that the considerable uncertainties in all salinity drivers together with the different responses
511 to these drivers cause the variability in the salinity projections. In our study, ICHEC and MPI models for RCP4.5 and
512 ICHEC for RCP8.5 showed no trends suggesting that it is very difficult to project the changes in the future. Worth
513 noting that single model projections of the saline water inflows from the North Sea to the Baltic Sea that can influence
514 the saline water intrusions to the Curonian Lagoon were not analyzed. However, given the significant increase in river
515 discharge is anticipated, the saltwater intrusion into the freshwater system is not likely.

516 **4.3 Water temperature and ice regime in the Curonian Lagoon**

517 All models showed a significantly increasing trend for the water temperatures with the highest rate of change for the
518 MOHC model and the lowest change for the MPI model. The analysis of the SD values strongly suggests that water
519 temperature is the most certain parameter and all models agree with the rise of water temperature. In general, all of
520 the Baltic Sea displays the same trends under RCP4.5 and 8.5 projections: the water temperature will increase, and
521 the sea-ice cover extent will decrease (Meier et al., 2022b). The impact of the increased water temperatures will be
522 mostly visible during winter periods and crucial for the coldwater species. We did not analyze the possible upwelling
523 and marine heatwave events that are important for the summer period and can have a significant influence on the
524 ecological status of the lagoon and southern Baltic Sea coasts, which leaves opportunity for future research directions.
525 Ice-related parameter results suggest a consistent and significant decline in ice season duration and maximum ice
526 thickness across multiple climate models and scenarios. Results are in line with Jakimavičius et al. (2020) study
527 accomplished with statistical methods using MPI, MOHC, and ICHEC model inputs for the Curonian Lagoon, where
528 the ice duration was projected to last 35–45 days for RCP4.5 and 3–34 for RCP8.5 with an expected decline of the ice
529 thickness up to 0–13 cm in the long term analysis. In our study, the highest rates of change were expressed by the
530 IPSL model, which was not included in the previous study. Nevertheless, both studies agreed that in the future the ice-
531 covered season will be shorter or even absent (RCP8.5). Decreasing ice cover will affect WRTs (Idzelytė et al., 2023a,
532 2020) and will have consequences for the lagoon ecosystem.

533 **4.4 Implications for nutrient load management**

534 One of the greatest concerns of the environmental managers is the projection of the river nutrient loads into the
535 Curonian Lagoon, which heavily affects eutrophication (Vybernaite-Lubiene et al., 2018, Stakėnienė et al., 2023).

536 This task also relates to the international commitment to reduce nutrient inputs into the Baltic Sea. According to our
537 model results (ICHEC, IPSL, MPI), the TP threshold could be achieved during several periods with fluctuating
538 patterns throughout the entire century if RCP4.5 scenario forcing is ensured. However, a severe discrepancy from the
539 targeted loads of TN is projected by the middle of the century by all models and especially by MOHC, regardless of
540 the RCP scenario. Despite the limitations of this study (i.e., not taking the possible land use and management change
541 into account), a worrying trend emerges with the increasing risk that with current regulations Lithuania will unlikely
542 meet the nutrient input ceilings defined in the HELCOM Baltic Sea Action Plan during the century.
543 Some studies demonstrate that future socioeconomic pathways could have a greater effect than climate change on
544 nutrients inputs to the Baltic Sea (Bartošová et al., 2019). Thus, the policy decisions within the BSAP framework do
545 not lose their importance, even in the context of climate-induced negative consequences, i.e., climate driven increase
546 in N loads. Measures designed and implemented can have a significant impact on environmental management
547 achievements of the threshold targets, especially if combined with emission reduction policy and socio-economic
548 transition towards more sustainable food and waste systems.

549 **4.5. Implications for nature protection and conservation**

550 Our study of climate change prediction uncertainty demands a re-evaluation of past approaches in biodiversity
551 conservation, highlighting the need for adaptive strategies in this field. Burbot used to be a significant part of the
552 commercial fish catch in the Curonian Lagoon before the 1990s and still is a very important target for game fishing,
553 especially under the ice. However, both commercial and recreational catches have fallen, and despite massive
554 restocking efforts, the stock is not improving. Some authors hypothesized that the main reason for the population
555 decline is the warming temperatures during the reproduction season (Švagždys, 2002). According to Skersonas et al.
556 (unpublished report 2019), the fall in catches of burbot in the Curonian Lagoon also coincided with the collapse of the
557 USSR and uncontrolled fishing at the beginning of the state's creation. According to our analysis, the stock collapse
558 period in fact corresponds to the presence of temperature changepoint detected in 1994, 1997, and 1992 in different
559 modeled data sets MPI, IPSL, and ICHEC, respectively. High variance of cold days duration among years during the
560 historic period was reflected in burbot stocks, the sequence of four to six cold winters was followed by a three to five-
561 fold increase in burbot catches (Švagždys, 2002). However, along with increasing temperature in the future, the change
562 between colder and warmer winters is not likely. The absence of ice cover, shift in spring flood timing, and increasing
563 water temperatures potentially could have implications for fish spawning phenology and spawning habitat quality.
564 Multiple changepoint detection analysis results showed a significant increase in temperature and shortening of the
565 cold period starting from the 1990s, indicating the onset of global warming. Assuming 'business as usual' carbon
566 emission scenario RCP8.5, the next notable decrease in cold period duration, already happened in 2023 (IPSL) or is
567 happening soon in 2025 (MPI) and 2030 (ICHEC). Thereafter the cold period lasts for as long as one month. Assuming
568 the emission reduction scenario RCP4.5, i.e., the stabilization of temperature trend, a one-month cold period duration
569 could be expected to last to the end of the century, according to MPI and ICHEC model results. However, IPSL results,
570 and especially MOHC results show no improvement even under the climate change mitigation scenario. Loss of ice
571 and cold isothermal conditions for spawning and egg development would further contribute to a significant decline in

572 burbot population natural recruitment. The aquaculture-based restocking as a conservation measure rather than a stock
573 improvement measure would become realistic in the near future.

574 **5 Conclusions and recommendations**

575 This study evaluates the output from various climate models to understand hydrological and hydrodynamic changes
576 in the Nemunas River, Curonian Lagoon, and southeastern Baltic Sea continuum under different climate change
577 scenarios. It highlights the importance of employing multiple models due to their unique predictions and the inherent
578 variability and complexity in projecting climate impacts on the analyzed hydrological and hydrodynamic parameters.
579 The analysis revealed that each model exhibits its own unique variability across all the examined parameters, while
580 some models show greater degrees of change, others are more stable. Yet, despite these variances, all models
581 consistently align in their projections and tendencies under the RCP4.5 and RCP8.5 climate change scenarios.

582 To summarize, the effective management of the Nemunas River – Curonian Lagoon – Baltic Sea continuum in a
583 changing climate needs a collaborative policy framework. Cross-sectoral working groups, focused on specific
584 challenges like nutrient management, should combine expertise from agriculture, water resources, and environmental
585 protection agencies. Engaging multiple stakeholder groups (fishermen, environmental managers, agricultural advisors,
586 scientists, policymakers, etc.) in designing and implementing climate-resilient practices fosters knowledge sharing
587 and feedback loops, leading to more effective and socially-accepted solutions. For example, promoting practices that
588 improve nutrient retention can also reduce runoff and, in turn, reduce the risk or magnitude of floods and protect
589 biodiversity.

590 With our study we strongly support development of predictive tools to aid in decision-making, risk assessment and
591 management. The variability results provide valuable insights to initiate policy updates, enhanced regional cooperation
592 and coordination, development of climate change indicators and associated revision of national monitoring programs
593 (e.g., Rose et al., 2023). Our results suggest that much greater efforts to mitigate global climate change are needed to
594 avoid high costs and difficulties to implement local climate mitigation measures.

595 **Data availability**

596 All numerical modeling results are openly available in the Zenodo open data repository
597 (<https://doi.org/10.5281/zenodo.7500744>, Idzelytė et al. (2023b)), initially generated in Idzelytė et al. (2023a) and
598 cited in this manuscript.

599 **Author contribution**

600 GU and NC initiated the conceptualization and funding acquisition of the research project. NC, JM and RI performed
601 the analysis and drafted the paper. RI, NC, JM and JL worked on the visualization of the results. NC, JM, RI prepared

602 the original manuscript draft with the assistance of JL, GU and AE. All co-authors reviewed the paper and contributed
603 to the scientific interpretation and discussion.

604 **Competing interests**

605 The authors declare that they have no conflict of interest.

606 **Acknowledgements**

607 This project has received funding from the Research Council of Lithuania (LMTLT), agreement No S-MIP-21-24.

608 **References**

- 609 Ashton, N. K., Jensen, N. R., Ross, T. J., Young, S. P., Hardy, R. S., and Cain, K. D.: Temperature and Maternal Age
610 Effects on Burbot Reproduction, *North Am. J. Fish. Manage.*, 39, 1192–1206, <https://doi.org/10.1002/nafm.10354>,
611 2019.
- 612 Akstinas, V., Jakimavičius, D., Meilutytė-Lukauskienė, D., Kriaučiūnienė, J., and Šarauskienė, D.: Uncertainty of
613 annual runoff projections in Lithuanian rivers under a future climate, *Hydrol. Res.*, 51(2), 257–271,
614 <https://doi.org/10.2166/nh.2019.004>, 2019.
- 615 Bartošová, A., Capell, R., Olesen, J. E., Jabloun, M., Refsgaard, J. C., Donnelly, C., Hyytiäinen, K., Pihlainen, S.,
616 Zandersen, M., and Arheimer, B.: Future socioeconomic conditions may have a larger impact than climate change on
617 nutrient loads to the Baltic Sea, *Ambio*, 48, 1325–1336, <https://doi.org/10.1007/s13280-019-01243-5>, 2019.
- 618 Blöschl, G., Hall, J., Parajka, J., Perdigao, R.A., Merz, B., Arheimer, B., et al.: Changing climate shifts timing of
619 European floods. *Science*, 357, 588-590, <https://doi.org/10.1126/science.aan2506>, 2017.
- 620 Chen, C., Gan, R., Feng, D., Yang, F., and Zuo, Q.: Quantifying the contribution of SWAT modeling and CMIP6
621 inputting to streamflow prediction uncertainty under climate change, *J. Clean. Prod.*, 364, 132675,
622 <https://doi.org/10.1016/j.jclepro.2022.132675>, 2022.
- 623 Čerkasova, N., Umgiesser, G., and Ertürk, A.: Development of a
624 hydrology and water quality model for a large transboundary river watershed to investigate the impacts of climate
625 change – A SWAT application, *Ecol. Eng.*, 124, 99–115, <https://doi.org/10.1016/j.ecoleng.2018.09.025>, 2018.
- 626 Čerkasova, N., Umgiesser, G., and Ertürk, A.: Assessing Climate Change Impacts on Streamflow, Sediment and
627 Nutrient Loadings of the Minija River (Lithuania): A Hillslope Watershed Discretization Application with High-
628 Resolution Spatial Inputs, *Water*, 11, 676, <https://doi.org/10.3390/w11040676>, 2019.
- 629 Čerkasova, N., Umgiesser, G., and Ertürk, A.: Modelling framework for flow, sediments and nutrient loads in a large
630 transboundary river watershed: A climate change impact assessment of the Nemunas River watershed, *J. Hydrol.*, 598,
631 126422, <https://doi.org/10.1016/j.jhydrol.2021.126422>, 2021.
- 632 Daggupati, P., Pai, N., Ale, S., Douglas-Mankin, K.R., Zeckoski, R.W., Jeong, J., Parajuli, P.B., Saraswat, D.,
633 Youssef, M.A.: A recommended calibration and validation strategy for hydrologic and water quality models.
Transactions of the ASABE, 58(6), 1705-1719, <https://doi.org/10.13031/trans.58.10712>, 2015.

634 Feyereisen, G., W., Strickland, T., C., Bosch, D., D., Sullivan, D., G.: Evaluation of SWAT manual calibration and
635 input parameter sensitivity in the Little River watershed. *Transactions of the ASABE*, 50(3), 843-855, 2007.

636 Foley, A.: Uncertainty in regional climate modeling: A review, *Prog. Phys. Geogr.: Earth Environ.*, 34(5), 647–670,
637 <https://doi.org/10.1177/0309133310375654>, 2010.

638 Gupta, R., Bhattarai, R., and Mishra, A.: Development of Climate Data Bias Corrector (CDBC) Tool and Its
639 Application over the Agro-Ecological Zones of India, *Water*, 11, 1102, <https://doi.org/10.3390/w11051102>, 2019.

640 Harrison, P. M., Gutowsky, L. F. G., Martins, E. G., Patterson, D. A., Cooke, S. J., and Power, M.: Temporal plasticity
641 in thermal-habitat selection of burbot *Lota lota* a diel-migrating winter-specialist, *Fish Biol.*, 88, 6: 2095–2308,
642 <https://doi.org/10.1111/jfb.12990>, 2016.

643 HELCOM: The revised nutrient input ceilings to the BSAP update, Helsinki Commission – HELCOM, Available
644 online at: <https://helcom.fi/wp-content/uploads/2021/10/Nutrient-input-ceilings-2021.pdf>, 2021.

645 Hussain, M., and Mahmud, I.: pyMannKendall: a python package for nonparametric Mann Kendall family of trend
646 tests, *J. Open Source Softw.*, 4, 1556, <https://doi.org/10.21105/joss.01556>, 2019.

647 Idzelytė, R., Čerkasova, N., Mėžinė, J., Dabulevičienė, T., Razinkovas-Baziukas, A., Ertürk, A., and Umgiesser, G.:
648 Coupled hydrological and hydrodynamic modeling application for climate change impact assessment in the Nemunas
649 river watershed–Curonian Lagoon–southeastern Baltic Sea continuum, *Ocean Sci.*, 19(4), 1047–1066,
650 <https://doi.org/10.5194/os-19-1047-2023>, 2023a.

651 Idzelytė, R., Čerkasova, N., Mėžinė, J., Dabulevičienė, T., Razinkovas-Baziukas, A., Ertürk, A., and Umgiesser, G.:
652 The computation results of coupled hydrological and hydrodynamic modelling application for the Nemunas River
653 watershed – Curonian Lagoon – South-Eastern Baltic Sea continuum, Zenodo [data set],
654 <https://doi.org/10.5281/zenodo.7500744>, 2023b.

655 Idzelytė, R. and Umgiesser, G.: Application of an ice thermodynamic model to a shallow freshwater lagoon, *Boreal*
656 *Environ. Res.*, 26, 61–77, 2021. Idzelytė, R., Mėžinė, J., Zemlys, P., and Umgiesser, G.: Study of ice cover impact on
657 hydrodynamic processes in the Curonian Lagoon through numerical modeling, *Oceanologia*, 62, 428–442,
658 <https://doi.org/10.1016/j.oceano.2020.04.006>, 2020.

659 Inácio, M., Schernewski, G., Nazemtseva, Y., Baltranaitė, E., Friedland, R., and Benz, J.: Ecosystem services
660 provision today and in the past: a comparative study in two Baltic lagoons, *Ecol. Res.*, 33, 1255–1274,
661 <https://doi.org/10.1007/s11284-018-1643-8>, 2018.

662 IPCC, 2013: Climate Change 2013: The Physical Science Basis. Contribution of Working Group I to the Fifth
663 Assessment Report of the Intergovernmental Panel on Climate Change [Stocker, T.F., Qin, D., Plattner, G.-K., Tignor,
664 M., Allen, S.K., Boschung, J., Nauels, A., Xia, Y., Bex, V., and Midgley, P.M. (eds.)]. Cambridge University Press,
665 Cambridge, United Kingdom and New York, NY, USA, 1535 pp., <https://doi.org/10.1017/CBO9781107415324>,
666 2013.

667 Ivanauskas, E., Skersonas, A., Andrašūnas, V., Elyaagoubi, S., and Razinkovas-Baziukas, A.: Mapping and Assessing
668 Commercial Fisheries Services in the Lithuanian Part of the Curonian Lagoon, *Fishes*, 7, 19,
669 <https://doi.org/10.3390/fishes7010019>, 2022.

670 Jakimavičius, D., Kriaučiūnienė, J., and Šarauskiene, D.: Impact of climate change on the Curonian Lagoon water
671 balance components, salinity and water temperature in the 21st century, *Oceanologia*, 60, 378–389,
672 <https://doi.org/10.1016/j.oceano.2018.02.003>, 2018.

673 Jakimavičius, D., Šarauskiene, D., and Kriaučiūnienė, J.: Influence of climate change on the ice conditions of the
674 Curonian Lagoon, *Oceanologia*, 62(2), 164–172, <https://doi.org/10.1016/j.oceano.2019.10.003>, 2020.

675 Kaziukonytė, K., Lesutienė, J., Gasiūnaitė, Z. R., Morkūnė, R., Elyaagoubi, S., and Razinkovas-Baziukas, A.: Expert-
676 Based Assessment and Mapping of Ecosystem Services Potential in the Nemunas Delta and Curonian Lagoon Region,
677 Lithuania, *Water*, 13(19), 2728, <https://doi.org/10.3390/w13192728>, 2021.

678 Killick, R., and Eckley, I. A.: changepoint: An R Package for Change-point Analysis, *J. Stat. Softw.*, 58(3), 1–19,
679 <https://www.jstatsoft.org/article/view/v058i03>, 2014.

680 Killick, R., Haynes, K., and Eckley, I. A.: changepoint: An R package for change-point analysis, R package version
681 2.2.4, <https://CRAN.R-project.org/package=changepoint>, 2022.

682 Latif, M.: Uncertainty in climate change projections, *J. Geochem. Explor.*, 110(1), 1–7,
683 <https://doi.org/10.1016/j.gexplo.2010.09.011>, 2011.

684 Lenderink, G., Buishand, A., and van Deursen, W.: Estimates of future discharges of the river Rhine using two
685 scenario methodologies: direct versus delta approach, *Hydrol. Earth Syst. Sci.*, 11, 1145–1159,
686 <https://doi.org/10.5194/hess-11-1145-2007>, 2007.

687 Lehner, F., Deser, C., Maher, N., Marotzke, J., Fischer, E. M., Brunner, L., and Hawkins, E.: Partitioning climate
688 projection uncertainty with multiple large ensembles and CMIP5/6, *Earth Syst. Dynam.*, 11(2), 491–508,
689 <https://doi.org/10.5194/esd-11-491-2020>, 2020.

690 Lin, B., Chen, X., Yao, H., Chen, Y., Liu, M., Gao, L., and James, A.: Analyses of landuse change impacts on
691 catchment runoff using different time indicators based on SWAT model, *Ecol. Indic.*, 58, 55–63,
692 <https://doi.org/10.1016/j.ecolind.2015.05.031>, 2015.

693 Lu, Y., Yuan, J., Lu, X., Su, C., Zhang, Y., Wang, C., Cao, X., Li, Q., Su, J., Ittekkot, V., Garbutt, R. A., Bush, S.,
694 Fletcher, S., Wagey, T., Kachur, A., and Sweijd, N.: Major threats of pollution and climate change to global coastal
695 ecosystems and enhanced management for sustainability, *Environ. Pollut.*, 239, 670–680,
696 <https://doi.org/10.1016/j.envpol.2018.04.016>, 2018.

697 Madec, G., and NEMO System Team: NEMO ocean engine, *Sci. Notes Clim. Model. Cent.*, 27, ISSN 1288-1619,
698 Institut Pierre-Simon Laplace (IPSL), 2004.

699 Marotzke, J., Giering, R., Zhang, K. Q., Stammer, D., Hill, C., Lee, T.: Construction of the adjoint MIT ocean general
700 circulation model and application to Atlantic heat transport sensitivity. *Journal of Geophysical Research: Oceans*, 104,
701 29529–29547, <https://doi.org/10.1029/1999JC900236>, 1999.

702 Meier, H. E. M., Kniebusch, M., Dieterich, C., Gröger, M., Zorita, E., Elmgren, R., Myrberg, K., Ahola, M. P.,
703 Bartosova, A., Bonsdorff, E., Börgel, F., Capell, R., Carlén, I., Carlund, T., Carstensen, J., Christensen, O. B.,
704 Dierschke, V., Frauen, C., Frederiksen, M., Gaget, E., Galatius, A., Haapala, J. J., Halkka, A., Hugelius, G., Hünicke,
705 B., Jaagus, J., Jüssi, M., Käyhkö, J., Kirchner, N., Kjellström, E., Kulinski, K., Lehmann, A., Lindström, G., May, W.,
706 Miller, P. A., Mohrholz, V., Müller-Karulis, B., Pavón-Jordán, D., Quante, M., Reckermann, M., Rutgersson, A.,

707 Savchuk, O. P., Stendel, M., Tuomi, L., Viitasalo, M., Weisse, R., and Zhang, W.: Climate change in the Baltic Sea
708 region: a summary, *Earth Syst. Dyn.*, 13, 457–593, <https://doi.org/10.5194/esd-13-457-2022>, 2022a.

709 Meier, H. E. M., Dieterich, C., Gröger, M., Dutheil, C., Börgel, F., Safonova, K., Christensen, O. B., and Kjellström,
710 E.: Oceanographic regional climate projections for the Baltic Sea until 2100, *Earth Syst. Dyn.*, 13, 159–199,
711 <https://doi.org/10.5194/esd-13-159-2022>, 2022b.

712 Mellor, G. L.: Users guide for a three-dimensional primitive equation numerical ocean model, Princeton Univ.,
713 Princeton, NJ, 08544–10710, 2004.

714 Neitsch, S. L., Arnold, J. G., Kiniry, J. R., and Williams, J. R.: Soil and Water Assessment Tool Theoretical
715 Documentation Version 2009, Texas Water Resources Institute, College Station, Texas, 2009.

716 Plunge, S., Gudas, M. and , Povilaitis, A.: Expected climate change impacts on surface water bodies in Lithuania,
717 *Ecohydrol. Hydrobiol.*, 22(2), 246–268, <https://doi.org/10.1016/j.ecohyd.2021.11.004>, 2022.

718 Rose, K.C., Bierwagen, B., Bridgham, S.D. et al. Indicators of the effects of climate change on freshwater ecosystems.
719 *Clim. Change* 176, 23, <https://doi.org/10.1007/s10584-022-03457-1>, 2023.

720 Song, Y. H., Chung, E. S., and Shiru, M. S.: Uncertainty Analysis of Monthly Precipitation in GCMs Using Multiple
721 Bias Correction Methods under Different RCPs, *Sustainability*, 12(18), 7508, <https://doi.org/10.3390/su12187508>,
722 2020.

723 Shchepetkin A.F., McWilliams, J.C.: The regional oceanic modeling system (ROMS): a split-explicit, free-surface,
724 topography-following-coordinate oceanic model. *Ocean Modelling*, 9 (4), 347–404,
725 <https://doi.org/10.1016/j.ocemod.2004.08.002>, 2005.

726 Stakėnienė, R., Jokšas, K., Kriaučiūnienė, J., Jakimavičius, D., Raudonytė-Svirbutavičienė, E.: Nutrient Loadings and
727 Exchange between the Curonian Lagoon and the Baltic Sea: Changes over the Past Two Decades (2001–2020), *Water*,
728 15, 4096, <https://doi.org/10.3390/w15234096>, 2023.

729 Stapanian, M. A., Paragamian, V. L., Madenjian, C. P., Jackson, J. R., Lappalainen, J., Evenson, M. J., and Neufeld,
730 M. D.: Worldwide status of burbot and conservation measures, *Fish Fish.*, 11(1), 34–56,
731 <https://doi.org/10.1111/j.1467-2979.2009.00340.x>, 2010.

732 Švagždys, A.: Growth and abundance of burbot in the Curonian Lagoon and determinatives of burbot abundance, *Acta*
733 *Zool. Lit.*, 12(1), 58–64, <https://doi.org/10.1080/13921657.2002.10512487>, 2002.

734 Taylor, K. E., Stouffer, R. J., and Meehl, G. A.: An Overview of CMIP5 and the Experiment Design, *Bull. Amer.*
735 *Meteor. Soc.*, 93(4), 485–498, <https://doi.org/10.1175/bams-d-11-00094.1>, 2012.

736 Tedesco, L., Vichi, M., Haapala, J., and Stipa, T.: An enhanced sea-ice thermodynamic model applied to the Baltic
737 Sea, *Boreal Environ. Res.*, 14, 68–80, 2009.

738 Tegegne, G., Melesse, A. M., and Worqlul, A. W.: Development of multi-model ensemble approach for enhanced
739 assessment of impacts of climate change on climate extremes, *Sci. Total Environ.*, 704, 135357,
740 <https://doi.org/10.1016/j.scitotenv.2019.135357>, 2020.

741 Umgiesser, G., Melaku Canu, D., Cucco, A., Solidoro, C.: A finite element model for the Venice Lagoon.
742 Development, set up, calibration and validation. *J. Mar. Sys.*, 51, 123–145,
743 <https://doi.org/10.1016/j.jmarsys.2004.05.009>, 2004.

744 Umgiesser, G., Ferrarin, C., Cucco, A., De Pascalis, F., Bellafiore, D., Ghezzi, M., and Bajo, M.: Comparative
745 hydrodynamics of 10 Mediterranean lagoons by means of numerical modeling, *J. Geophys. Res. Oceans*, 119, 2212–
746 2226, <https://doi.org/10.1002/2013JC009512>, 2014.

747 Umgiesser, G., Zemlys, P., Erturk, A., Razinkova-Baziukas, A., Mežine, J., and Ferrarin, C.: Seasonal renewal time
748 variability in the Curonian Lagoon caused by atmospheric and hydrographical forcing, *Ocean Sci.*, 12(2), 391–402,
749 <https://doi.org/10.5194/os-12-391-2016>, 2016.

750 Viitasalo, M. and Bonsdorff, E.: Global climate change and the Baltic Sea ecosystem: direct and indirect effects on
751 species, communities and ecosystem functioning, *Earth Syst. Dynam.*, 13, 711–747, [https://doi.org/10.5194/esd-13-](https://doi.org/10.5194/esd-13-711-2022)
752 711-2022, 2022.

753 Vybernaite-Lubiene, I., Zilius, M., Saltyte-Vaisiauske, L., and Bartoli, M.: Recent Trends (2012–2016) of N, Si, and
754 P Export from the Nemunas River Watershed: Loads, Unbalanced Stoichiometry, and Threats for Downstream
755 Aquatic Ecosystems, *Water*, 10, 1178, <https://doi.org/10.3390/w10091178>, 2018.

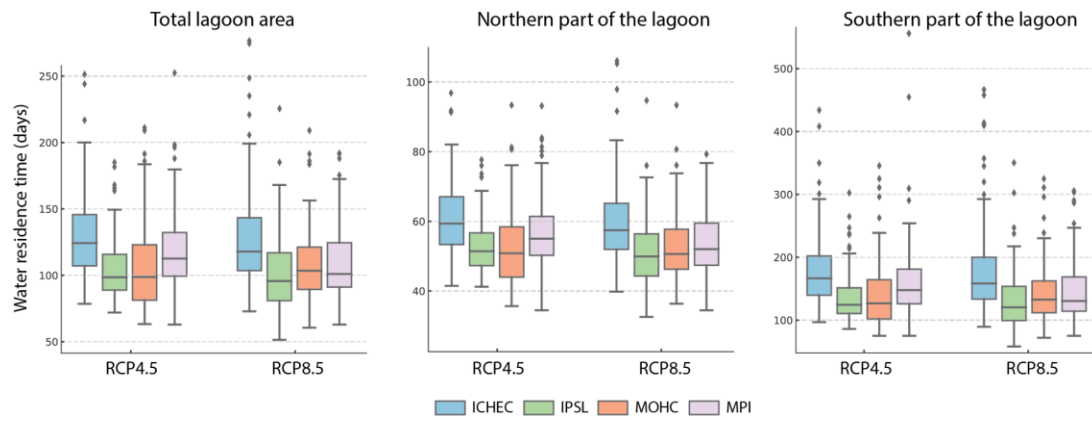
756 Waikhom, S. I., Yadav, V., Azamathulla, H. M., and Solanki, N.: Impact assessment of land use/land cover changes
757 on surface runoff characteristics in the Shetrunji River Basin using the SWAT model, *Water Pract. Tech.*, 18(5), 1221–
758 1232, <https://doi.org/10.2166/wpt.2023.071>, 2023.

759 Wang, G., Yang, H., Wang, L., Xu, Z., and Xue, B.: Using the SWAT model to assess impacts of land use changes
760 on runoff generation in headwaters, *Hydrol. Processes*, 28(3), 1032–1042, <https://doi.org/10.1002/hyp.9645>, 2012.

761 Zemlys, P., Ferrarin, C., Umgiesser, G., Gulbinskas, S., and Bellafiore, D.: Investigation of saline water intrusions
762 into the Curonian Lagoon (Lithuania) and two-layer flow in the Klaipeda Strait using finite element hydrodynamic
763 model, *Ocean Sci.*, 9, 573–584, <https://doi.org/10.5194/os-9-573-2013>, 2013.

764

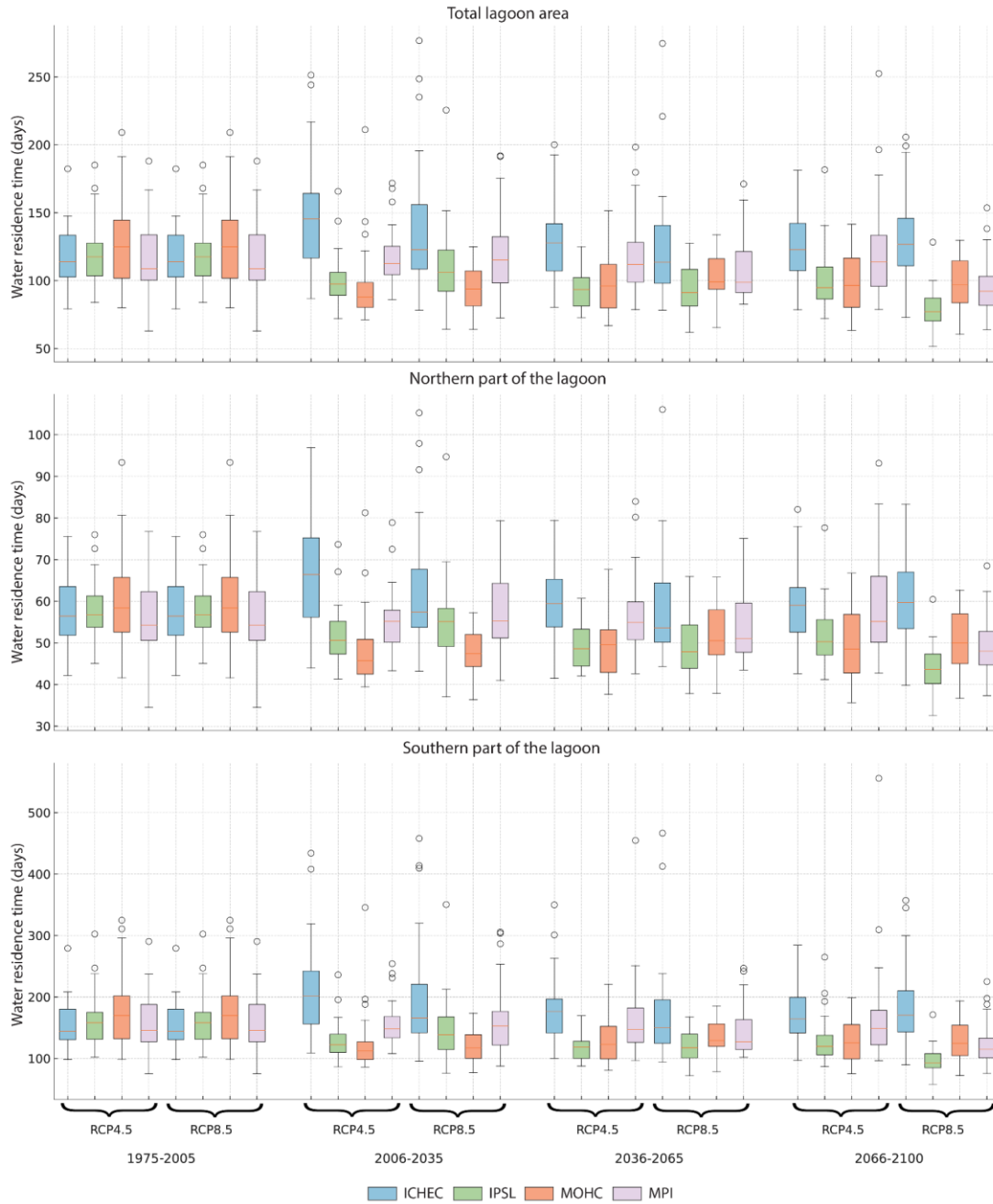
765 **Appendix A: Additional results of the water residence time**



766

767 **Figure A1. Annual average water residence time (in days) in the total lagoon area, as well as separately -**

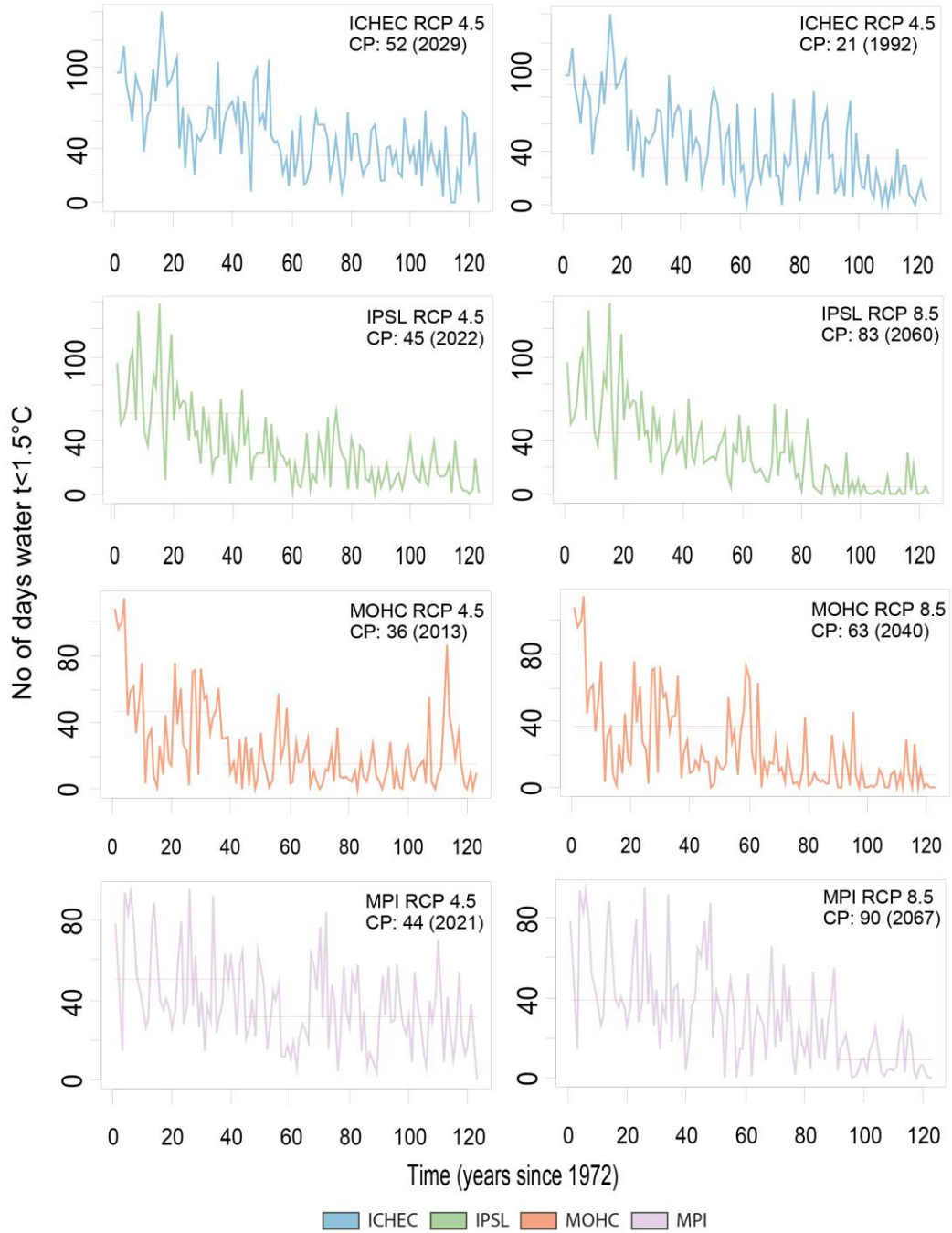
768 **northern and southern parts of it, under RCP4.5 (left column) and RCP8.5 (right column) scenarios.**



769
770
771
772

Figure A2. Average water residence time (in days) in the total lagoon area, northern and southern parts under RCP4.5 (left column) and RCP8.5 (right column) scenarios splitted to 30 years periods.

773 **Appendix B: Results of the changepoint analysis**

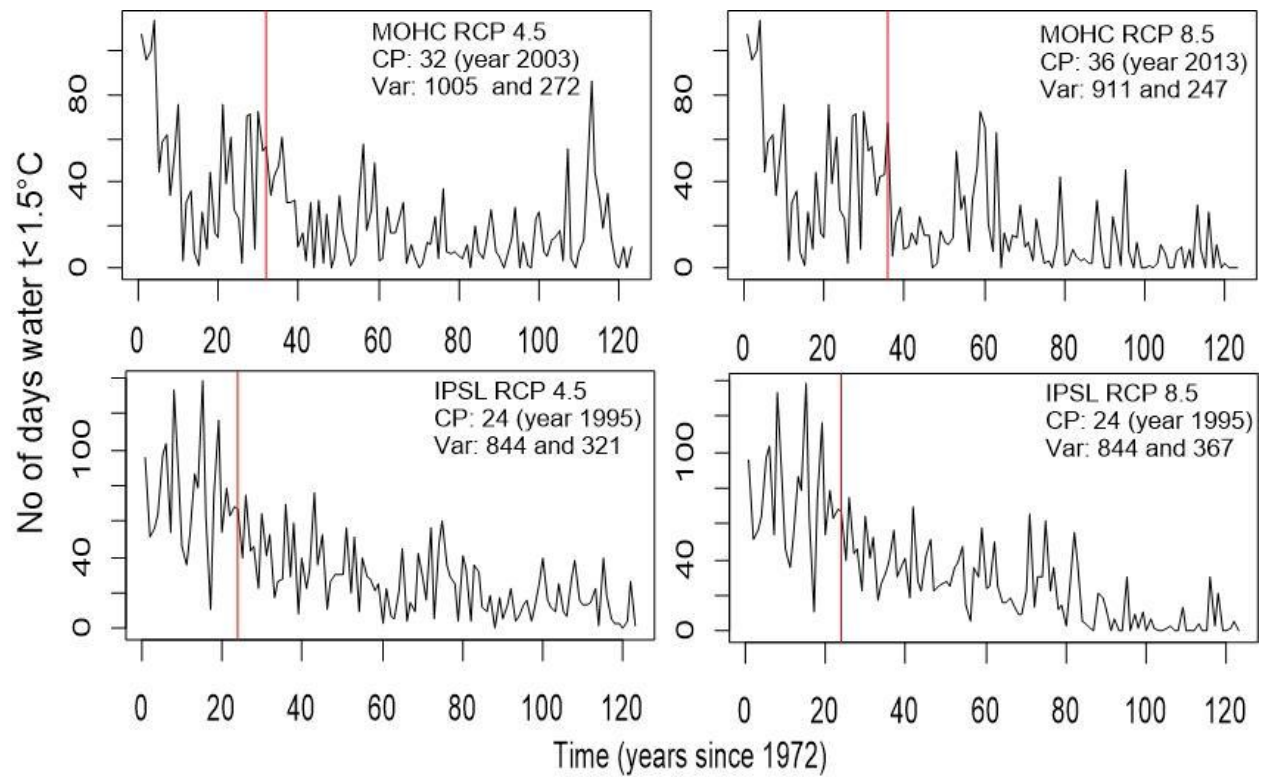


774

775 **Figure B1. Single change point (CP) detection in the modeled time series of burbot spawning period $t < 1.5^\circ\text{C}$ duration (Vente**

776 **area). Means (M) and variances (V) of two periods are provided.**

777



778

779 **Figure B2. Single change point (CP) of variances detection in the modeled time series of burbot spawning period $t < 1.5^{\circ}\text{C}$**
 780 **duration (Vente area). Variances (Var) of two periods are provided.**

781